

# Ancient horse genomes reveal the timing and extent of dispersals across the Bering Land Bridge

Alisa O. Vershinina<sup>1</sup>  | Peter D. Heintzman<sup>2</sup>  | Duane G. Froese<sup>3</sup> | Grant Zazula<sup>4,5</sup> | Molly Cassatt-Johnstone<sup>1</sup> | Love Dalén<sup>6,7</sup>  | Clio Der Sarkisian<sup>8</sup> | Shelby G. Dunn<sup>1</sup> | Luca Ermini<sup>9</sup>  | Cristina Gamba<sup>9</sup> | Pamela Groves<sup>10</sup> | Joshua D. Kapp<sup>1</sup> | Daniel H. Mann<sup>10</sup> | Andaine Seguin-Orlando<sup>8</sup> | John Southon<sup>11</sup> | Mathias Stiller<sup>1,12</sup> | Matthew J. Wooller<sup>13,14</sup> | Gennady Baryshnikov<sup>15</sup> | Dmitry Gimranov<sup>16,17</sup> | Eric Scott<sup>18</sup> | Elizabeth Hall<sup>5</sup> | Susan Hewitson<sup>5</sup> | Irina Kirillova<sup>19</sup> | Pavel Kosintsev<sup>16</sup> | Fedor Shidlovsky<sup>20</sup> | Hao-Wen Tong<sup>21,22</sup> | Mikhail P. Tiunov<sup>23</sup> | Sergey Vartanyan<sup>24</sup> | Ludovic Orlando<sup>8</sup>  | Russell Corbett-Detig<sup>25</sup> | Ross D. MacPhee<sup>26</sup> | Beth Shapiro<sup>1,27</sup> 

<sup>1</sup>Ecology and Evolutionary Biology, University of California Santa Cruz, Santa Cruz, CA, USA

<sup>2</sup>The Arctic University Museum of Norway, UiT - The Arctic University of Norway, Tromsø, Norway

<sup>3</sup>Department of Earth and Atmospheric Sciences, University of Alberta, Edmonton, AB, Canada

<sup>4</sup>Collections and Research, Canadian Museum of Nature, Station D, Ottawa, ON, Canada

<sup>5</sup>Government of Yukon, Department of Tourism and Culture, Palaeontology Program, Whitehorse, YT, Canada

<sup>6</sup>Department of Bioinformatics and Genetics, Swedish Museum of Natural History, Stockholm, Sweden

<sup>7</sup>Centre for Palaeogenetics, Stockholm, Sweden

<sup>8</sup>Centre d'Anthropobiologie et de Génomique de Toulouse UMR5288, Faculté de Médecine Purpan, Université Paul Sabatier, Toulouse, France

<sup>9</sup>Lundbeck Foundation GeoGenetics Center, University of Copenhagen, Copenhagen, Denmark

<sup>10</sup>Institute of Arctic Biology, University of Alaska Fairbanks, Fairbanks, CA, USA

<sup>11</sup>Keck-CCAMS Group, Earth System Science Department, University of California, Irvine, CA, USA

<sup>12</sup>Division Molecular Pathology, Institute of Pathology, University Hospital Leipzig, Leipzig, Germany

<sup>13</sup>Alaska Stable Isotope Facility, Water and Environmental Research Center, Institute of Northern Engineering, University of Alaska Fairbanks, Fairbanks, AK, USA

<sup>14</sup>Department of Marine Biology, College of Fisheries and Ocean Sciences, University of Alaska Fairbanks, Fairbanks, AK, USA

<sup>15</sup>Laboratory of Theriology, Zoological Institute of the Russian Academy of Sciences, St. Petersburg, Russia

<sup>16</sup>Institute of Plant & Animal Ecology of the Russian Academy of Sciences, Ural Branch, Ekaterinburg, Russia

<sup>17</sup>Ural Federal University named after the first President of Russia B. N. Yeltsin, Ekaterinburg, Russia

<sup>18</sup>California State University, San Bernardino, CA, USA

<sup>19</sup>Institute of Geography, Russian Academy of Sciences, Moscow, Russia

<sup>20</sup>National Alliance of Shidlovskiy "Ice Age," Moscow, Russia

<sup>21</sup>Key Laboratory of Vertebrate Evolution and Human Origins of Chinese Academy of Sciences, Institute of Vertebrate Paleontology and Paleoanthropology, Chinese Academy of Sciences, Beijing, China

<sup>22</sup>CAS Center for Excellence in Life and Palaeoenvironment, Chinese Academy of Sciences, Beijing, China

<sup>23</sup>Federal Scientific Center of the East Asia Terrestrial Biodiversity, Far Eastern Branch of Russian Academy of Sciences, Vladivostok, Russia

<sup>24</sup>North-East Interdisciplinary Scientific Research Institute N.A. Shilo, Far East Branch, Russian Academy of Sciences, Magadan, Russia

<sup>25</sup>Biomolecular Engineering, University of California Santa Cruz, Santa Cruz, CA, USA

<sup>26</sup>American Museum of Natural History, New York, NY, USA

<sup>27</sup>Howard Hughes Medical Institute, University of California Santa Cruz, Santa Cruz, CA, USA

**Correspondence**

Alisa O. Vershinina and Beth Shapiro,  
Ecology and Evolutionary Biology,  
University of California Santa Cruz, Santa  
Cruz, CA, USA  
Email: avershin@ucsc.edu (A.V.);  
bashpir@ucsc.edu (B.S.)

**Funding information**

Gordon & Betty Moore Foundation,  
Grant/Award Number: 3804; European  
Research Council, Grant/Award Number:  
681605; American Wild Horse Campaign;  
National Genomics Infrastructure funded  
by the Swedish Research Council; Uppsala  
Multidisciplinary Center for Advanced  
Computational Science; Knut och Alice  
Wallenbergs Stiftelse; U.S. Bureau of  
Land Management; Natural Science  
and Engineering Research Council of  
Canada; Svenska Forskningsrådet Formas,  
Grant/Award Number: 2018-01640;  
University of California, Santa Cruz; Cana  
Foundation; Science for Life Laboratory;  
Federal theme of Zoological Institute  
of the Russian Academy of Sciences,  
Grant/Award Number: AAAA-A19-  
119032590102-7; Russian Foundation for  
Basic Research, Grant/Award Number:  
18-04-00327 and 19-05-00477; NSF,  
Grant/Award Number: ARC-1417036; FP7,  
Grant/Award Number: IEF-302617

**Abstract**

The Bering Land Bridge (BLB) last connected Eurasia and North America during the Late Pleistocene. Although the BLB would have enabled transfers of terrestrial biota in both directions, it also acted as an ecological filter whose permeability varied considerably over time. Here we explore the possible impacts of this ecological corridor on genetic diversity within, and connectivity among, populations of a once wide-ranging group, the caballine horses (*Equus* spp.). Using a panel of 187 mitochondrial and eight nuclear genomes recovered from present-day and extinct caballine horses sampled across the Holarctic, we found that Eurasian horse populations initially diverged from those in North America, their ancestral continent, around 1.0–0.8 million years ago. Subsequent to this split our mitochondrial DNA analysis identified two bidirectional long-range dispersals across the BLB ~875–625 and ~200–50 thousand years ago, during the Middle and Late Pleistocene. Whole genome analysis indicated low levels of gene flow between North American and Eurasian horse populations, which probably occurred as a result of these inferred dispersals. Nonetheless, mitochondrial and nuclear diversity of caballine horse populations retained strong phylogeographical structuring. Our results suggest that barriers to gene flow, currently unidentified but possibly related to habitat distribution across Beringia or ongoing evolutionary divergence, played an important role in shaping the early genetic history of caballine horses, including the ancestors of living horses within *Equus ferus*.

**KEYWORDS**

Bering Land Bridge, *Equus ferus*, horses, palaeogenomics, population structure

**1 | INTRODUCTION**

The physiographic region of Beringia extends from the Lena River in Russia to the Mackenzie River in Canada and consists of both terrestrial and marine components (Figure 1a) (Hopkins, 1959). Beringia's land area varied during the Pleistocene (2.6 million [Ma] to 11.7 thousand [ka] years ago) along with the extent of continental ice and its effect on sea level (Elias & Brigham-Grette, 2013; Hopkins, 1973). Times of maximum subaerial exposure created a nearly continuous plain between Western (Asian) and Eastern (North American) Beringia, referred to as the Bering Land Bridge (BLB). At other times these regions were separated by the rejuvenated marine passage (Sher, 1999). Beringia therefore could have acted as either a conduit or a barrier for dispersing marine and terrestrial species (Alter et al., 2015; Guthrie, 1982; Hopkins, 1959; McKeon et al., 2016; Wooller et al., 2018; Zazula et al., 2014).

Barriers like the BLB can influence species' evolutionary trajectories by impeding or eliminating gene flow. Barriers may, for example, lead to allopatric speciation via genetic drift and local adaptation (Marques et al., 2019; Schield et al., 2019), or create opportunities for evolutionary innovation via subsequent admixture after barriers are removed (Coyne & Orr, 1998; Nosil & Feder, 2012; Payseur &

Rieseberg, 2016). The impact of barriers on species' evolution will, however, depend on their nature and permanency. In Beringia, the periodic inundation of the BLB created temporarily isolated continental populations of many wide-ranging terrestrial animals, including bison (*Bison* sp.), mammoths (*Mammuthus* sp.) and wolves (*Canis* sp.). Analyses of ancient mitochondrial DNA (mtDNA) from *Mammuthus*, *Bison* and *Canis* have revealed strong phylogeographical contrasts between the continents, presumably a consequence of the barrier imposed by intermittent inundation of the BLB (Chang et al., 2017; Froese et al., 2017; Loog et al., 2019; Lorenzen et al., 2011). Consistent with this structuring, all three mitochondrial data sets include evidence of multiple dispersals across the BLB. These data imply that gene flow may have regularly occurred between continental populations of different species at least periodically during the Pleistocene, a hypothesis amenable to further testing using nuclear genomic data sets.

The chronology of BLB availability as a terrestrial corridor for dispersal between Eurasia and North America remains poorly resolved. During the Pleistocene, ice volume and sea level estimates indicate that the BLB was largely exposed during Marine Isotope Stage (MIS) 6, ~190–130 ka; MIS 4, ~70–60 ka; and from middle MIS 3 to early MIS 1, ~45–11 ka (Hu et al., 2010; Jakobsson et al., 2017). The timing of

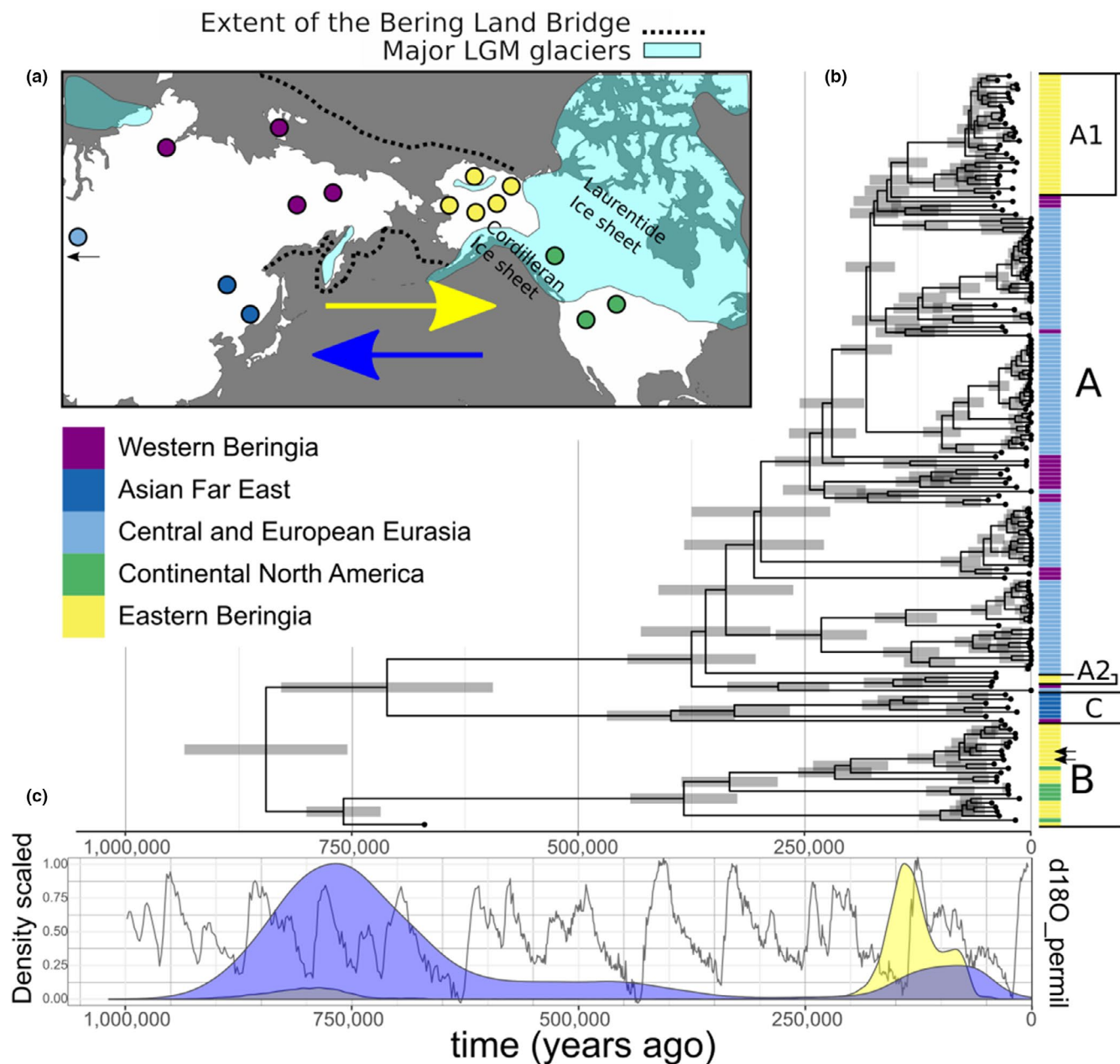


**FIGURE 1** Sampling locations and phylogeographical analysis of ancient and present-day caballine horse mitochondrial genomes. (a) Geographical distribution of the samples with palaeogeographical reconstruction of Beringia during the Last Glacial Maximum (LGM) ~25–23 ka (redrawn from Dyke, 2004). Arrows designate direction of dispersal modelled in the CTMC Markov jumps analysis. (b) Time-calibrated mitochondrial genealogy. Each sample was assigned to either Eurasia or North America based on their sampling location relative to the present-day Bering Strait. Grey bars represent the 95% highest probability density (HPD) interval of node heights. Arrows show positions of YG188.42 and YG303.325. We calibrated radiocarbon ages of the Late Pleistocene samples reported in Table S1 using the IntCal13 curve (Reimer et al., 2013) and OxCal version 4.2 (Ramsey, 2009), and assigned the median calibrated age of each sample as prior information. If a sample was dated using stratigraphic information (Fages et al., 2019), we assigned the mean of the tentative age interval as a date prior (Table S2). Samples without age information were excluded from the analysis. The version of the genealogy with tip labels is presented in Figure S3. (c) Density plots (scaled to 1) representing the timing of movements between Western and Eastern Beringia with  $\delta^{18}\text{O}$  values plotted on the second y-axis. Density colours indicate the direction of movement, following the arrows in (a). The  $\delta^{18}\text{O}$  curve is a proxy for global temperature and ice volume (Lisiecki & Raymo, 2005). [Colour figure can be viewed at [wileyonlinelibrary.com](http://wileyonlinelibrary.com)]

the BLB exposure prior to MIS 6 is obscure (see O'Regan et al., 2010). However, exposure of the BLB does not necessarily imply that the region was viable as an ecological corridor for megafauna. Marine transgression would have disrupted the continuity of the Mammoth Steppe

grassland and fragmented habitat available to large-bodied grazers (Guthrie, 2001; Lorenzen et al., 2011; Zimov et al., 2012). Habitat re-establishment following re-emergence of the BLB was probably impacted by variable sea levels, local climates and regional topography,

all of which varied across Beringia (Bond, 2019; Elias & Crocker, 2008; Knebel & Creager, 1973). The patchiness of habitat availability on the BLB would have facilitated some species' migrations while hampering others (Guthrie, 1982; Mann et al., 2015).

Reconstructions of first appearance dates (FADs) for different mammals dispersing across the BLB support the conclusion that optimal conditions for dispersal were intermittent and varied by taxon (Salis et al., 2020). The current North American FAD for mammoths, for example, is the Early Pleistocene, ~1.5 Ma (Lister & Sher, 2015), while bison first entered North America during MIS 6, ~195–135 ka, and then again at ~45–21 ka (Froese et al., 2017). If humans crossed over the BLB, as opposed to sailing along its southern coast, they may have done so at this later time as well (Moreno-Mayar et al., 2018). Moose (*Alces alces*) and wapiti (*Cervus elaphus*) expanded across the BLB into North America later, ~15 ka (Guthrie, 2006; Meiri et al., 2014, 2020). By contrast, there is no evidence that the woolly rhinoceros (*Coelodonta antiquitatis*) dispersed into North America at any time (Guthrie, 2001; Stuart & Lister, 2012).

Successful dispersals in the opposite direction were fewer, but an outstanding case is that of caballine horses (within Quaternary equid diversity, the horses most closely related to the extant domestic horse, *Equus caballus*). Caballine horses diverged from their sister group in North America ~4.5–4.0 Ma (Orlando et al., 2013), and their fossil record suggests that they had already dispersed into Eurasia by ~0.9–0.8 Ma (Azzaroli, 1989; Forstén, 1991). This timing is in good agreement with the most recent molecular estimate of the Eurasian FAD for caballines based on nuclear genomes (~1.06 Ma; Orlando et al., 2013). Although the North American caballine horse population would eventually become extinct during the early Holocene (Haile et al., 2009), caballines on either side of the BLB became widespread after the initial dispersal (MacFadden, 2005) and, in the case of one or more Eurasian populations, were eventually domesticated (Fages et al., 2019; Gaunitz et al., 2018; Orlando, 2020; Schubert et al., 2014).

Despite their extensive fossil record, much less is known compared to other megafaunal species about how often and in which direction caballine horses dispersed across the BLB. Previous phylogenetic analyses of part of the mitochondrial control region suggest that caballine horses dispersed back into North America from Asia at least once during the Pleistocene (Barrón-Ortiz et al., 2017; Weinstock et al., 2005). If this happened, this could provide an excellent opportunity to examine how alternating periods of isolation and connectivity might have affected the population biology of ancient horse populations on both sides of the BLB.

Here, we use palaeogenomic data from caballine horse remains collected in Eastern and Western Beringia as well as in temperate northeastern Asia and the mid-continental United States to explore the history of caballine horse dispersal across the BLB. We sequence and assemble two new caballine horse palaeogenomes from Yukon Territory, Canada, which represent the first high-coverage nuclear sequences for North American caballines, and 78 new mitochondrial genomes from caballine horses across Eurasia and North America. We then use these and previously published data (seven nuclear and 112 mitochondrial genomes) to explore the timing and nature

of caballine horse dispersal across the BLB and the potential for bi-directional gene flow among horse populations across the transient corridor.

## 2 | METHODS

### 2.1 | Sample collection, screening for DNA preservation and dating

We collected samples of 262 horse bones and teeth from Eurasia (Ural Mountains and Siberia, Russia; eastern China) and North America (Yukon Territory, Canada; Alaska, USA; continental USA) (Figure 1a; Table S1). Most horse remains analysed in this study have been attributed as *Equus* sp.; however, some have been assigned on morphological grounds to a variety of likely nominal species, including *Equus ferus*, *E. lambei*, *E. uralensis* and *E. przewalskii* (see Table S1). As species-level systematics of Holarctic equids is a subject of considerable debate (see Barron-Ortiz et al., 2019 for discussion), we avoid official species designations here.

We processed specimens following standard protocols for working with degraded DNA (Fulton & Shapiro, 2019) in dedicated ancient DNA facilities at the University of California Santa Cruz Paleogenomics Laboratory (PGL) or Center for GeoGenetics, University of Copenhagen, Denmark (CGG). For each specimen, we cleaned the surface to remove potential surface contaminants and then sampled ~1 g of bone powder for radiocarbon dating and genetic analyses (Table S1).

To extract DNA, we applied a sodium hypochlorite pretreatment to ~0.1 g of bone powder to remove external DNA contamination (Korlević & Meyer, 2019) and then followed one of several extraction methods optimized for ancient DNA (Dabney & Meyer, 2019; Rohland et al., 2010). We used several library preparation protocols and indexing protocols, including single- and double-stranded DNA library preparation (Kapp et al., 2020; Meyer & Kircher, 2010) and single- and dual-indexing strategies (Kircher et al., 2012). Sample-specific details are provided in Table S1. We sequenced each library on an Illumina MiSeq (2 × 75 cycles) or HiSeq (2 × 150 cycles) to a depth of 0.2–8.0 million reads, and screened samples by mapping recovered data to the EquCab2 reference genome as described below. Out of 262 samples, 78 had >1% endogenous DNA and a maximum of 1%–30% clonality, and we selected these for genetic analyses.

We sent 71 of the 78 well-preserved samples (seven were dated previously) for accelerator mass spectrometry (AMS) radiocarbon dating at either the Lawrence Livermore National Laboratory or the UC Irvine KECK AMS facilities (Appendix S1). All dates with the references for the published samples are provided in Tables 1 and S1.

### 2.2 | Mitochondrial genome assembly

Twenty of the 78 well-preserved samples yielded >4-fold coverage mitochondrial genomes from the screening data (Table S1). For the

TABLE 1 Ancient and present-day nuclear genomes analysed in this study.

Specimen ID	Nuclear genome coverage (fold)	Uncalibrated radiocarbon date	Calibrated age (years BP)	Radiocarbon facility ID	References
Batagai	18.3	4,450 ± 35	5,104 ± 109	Gr-50842	Librado et al., (2015)
CGG10022	24.3	38,565 ± 602	42,620 ± 440	UBA-16478	Schubert et al., (2014)*
CGG10023	7.4	13,389 ± 52	16,112 ± 96	UBA-16479	Schubert et al., (2014)*
YG303.325	25.9	26,020 ± 140	30,318 ± 245	CAMS-157454	This study
YG188.42/YT03-40	25.1	23,920 ± 100	27,947 ± 130	OxA-17686	This study**
YG148.20/TC21	0.7	–	~560,000–780,000	–	Orlando et al., (2013)*
Thoroughbred (Twilight)	21.0	–	Present-day	–	Orlando et al., (2013)
Przewalski (MK822)	9.1	–	Present-day	–	Orlando et al., (2013)
Donkey (Willy)	11.8	–	Present-day	–	Orlando et al., (2013)

Note: Coverage is reported based on alignment of whole genome data to the EquCab2.0 reference (Wade et al., 2009). Median and 1 sigma values are reported for dates calibrated with the IntCal13 curve as implemented in OxCal 4.3 (Ramsey, 2009; Reimer et al., 2013). Previously published radiocarbon and stratigraphic dates: \*Orlando et al., (2013); \*\*Lorenzen et al., (2011).

remaining 58, we performed RNA-bait hybridization-based target enrichment using the horse “myBaits Expert Mito” kit (Daicel Arbor Biosciences, previously MYcroarray) and following the manufacturer's protocols version 1 to version 4, with hybridization at 65°C for 36 hr as described by Vershinina et al., (2019). We sequenced the enriched libraries on an Illumina MiSeq (2 × 75 cycles). To assemble mitochondrial genomes, we used a bash script (mito\_assembly\_pipeline.sh) available from <https://github.com/Paleogenomics/DNA-Post-Processing/>. This pipeline trims adapters, merges reads overlapping by ≥15 bp, discards reads shorter than 27 bp with SEQPREP2 (<https://github.com/jeizenga/SeqPrep2>), and removes reads with low sequence complexity using PRINSEQ-LITE version 0.20.4 (Schmieder & Edwards, 2011) with the flag “dust = 7.” Merged and unmerged fastq files are concatenated and converted to fasta with the FASTX-TOOLKIT version 0.0.13.2 (Gordon, Hannon, & Others, 2010). We then assembled mitochondrial genomes using Mapping Iterative Assembler version 1.0 (MIA; <https://github.com/mpieva/mapping-iterative-assembler>) with the domestic horse mitochondrial genome (NC\_001640; Xu & Arnason, 1994) as the seed sequence. From the MIA assembly, we called bases at sites covered by at least three independent reads and for which we observed >67% consensus among reads. The 78 new mitochondrial genomes resulting from this pipeline are available at GenBank with accessions MW846090–MW846167.

We augmented our data set with 110 previously published ancient and present-day horse mitogenomes from across their Holarctic Pleistocene range (Fages et al., 2019; Librado et al., 2015; Lippold et al., 2011; see Table S2 for the complete list of references). Mitochondrial genomes from Fages et al., (2019) were published as BAM alignments. We converted these to fastq with BEDTOOLS version 2.25.0 bamtofastq (Quinlan & Hall, 2010) and re-assembled mitochondrial genomes following the pipeline above.

We added the donkey (*E. asinus*, GenBank: NC\_001788; Xu et al., 1996), Ovodov's horse and zebra (*E. ovodovi*: NC\_018783.1; *E. zebra*: NC\_020476.1; both Vilstrup et al., 2013) mitochondrial genomes to our data set and aligned all mitogenomes using MUSCLE version 3.8.425 (Edgar, 2004). We then manually inspected the alignment to correct

misaligned gaps. Our final alignment comprised 190 equid mitochondrial genomes, including three outgroup sequences (donkey, zebra, Ovodov's horse) and 187 caballine horses sampled from across the Holarctic and ranging in age from early–Middle Pleistocene (*E. cf. scotti*; Orlando et al., 2013) to the present (Figure 1; Tables S1 and S2).

### 2.3 | Mitochondrial phylogenetic analysis

We estimated mitochondrial phylogenies using three approaches. First, we used the maximum likelihood (ML) approach implemented in RAXML version 8.2.4 (Stamatakis, 2014) and the Bayesian time-calibrated approach implemented in BEAST version 1.10.1 (Suchard et al., 2018). In RAXML, we considered the alignment as one partition and ran three instances of RAXML assuming the GTRGAMMAI model of nucleotide substitution (Figure S1).

Next, we estimated the timing of divergence between caballine horse lineages using BEAST. We calibrated the molecular clock using median calibrated radiocarbon dates or mean stratigraphic age for each sample (Tables S1 and S2), excluding samples with nonfinite or no age estimates, and a prior at the root of the tree of 4.0–4.5 Ma (normal prior, mean 4.25 Ma, SD: 0.15 Ma) based on Orlando et al., (2013). We placed an additional normal prior on the age of the early–Middle Pleistocene Thistle Creek horse YG148.20/TC21 (GenBank: KT757763) with a mean of 670 ka and SD of 56.4 ka following the proposed range of this sample's age (560–780 ka BP; Orlando et al., 2013). We assumed the GTR+G nucleotide model with four rate categories and an uncorrelated log-normally distributed relaxed clock model with exponential prior 4.68E-8 (mean, substitutions per site per million years) (Schubert et al., 2014), and the Bayesian SkyGrid (Gill et al., 2013; Hill & Baele, 2019) coalescent prior with 150 groups. We ran two Markov chain Monte Carlo (MCMC) chains for 100 million iterations each, sampling parameters and trees every 10,000 states, discarded the first 25% as burn-in, combined the remainder using LOGCOMBINER version 1.10.4, and then analysed parameter convergence in TRACER version 1.7.1 (Rambaut

et al., 2018) (Table S4). We combined the posterior trees and calculated the maximum clade credibility (MCC) tree in TREEANNOTATOR version 1.10.4 (Rambaut & Drummond, 2010) (Figure S2).

Third, we used the continuous-time Markov chain (CTMC) (Minin & Suchard, 2008a, 2008b) to infer the timing and number of migrations across the BLB, using only dated caballine horses (Figure 1b,c). It has been previously shown that placement of various outgroups, or the lack thereof, affects phylogenetic position of horses from Far Eastern Asia and New Siberian Islands (Fages et al., 2019; Heintzman et al., 2017; Yuan et al., 2020). The deeply divergent clade probably forms a root polytomy, but appears to be more closely related to specimens from the rest of Eurasia. Through initial CTMC runs, we found that the polytomy problem was further exacerbated when the archaic Middle Pleistocene YG148.20/TC21 was included in the analysis. To account for the confounding effects of the polytomy on the unrooted CTMC BEAST run, we enforced two monophylies. One monophyly united samples from Far Eastern Asia and New Siberian Islands with the remaining Eurasian haplogroup horses. The second monophyly united samples with the North American haplogroup. We selected samples for both haplogroups based on our RAXML and BEAST analyses, which included noncaballine horses, and on previous studies (Yuan et al., 2020). We placed a normal prior of 850 ka ( $SD$ : 200 ka) on the root height of the tree based on Orlando et al., (2013).

For the CTMC analysis, we subdivided the mitochondrial alignment into four partitions: protein-coding genes (CDS), tRNA, rRNA and control region (CR), and removed the variable portion of the CR spanning 16,167–16,475 bp that cannot be assembled accurately from short reads (e.g., Heintzman et al., 2017). Following results of JMODELTEST version 2.1.10 (Darrriba et al., 2012), we assigned GTR+I+G to the CDS, CR and rRNA partitions and HKY+I+G to the tRNA partition, and assumed a strict molecular clock. We ran and analysed two MCMC chains and posterior trees with the same number of steps, burn-in and sampling parameters as in BEAST that included the outgroups as described above. We computed the density distribution of the geographical parameter with R version 4.0.2 (R Core Team, 2014). We used R packages GGRTREE (Yu et al., 2017), TREEIO (Wang et al., 2020) and GGLOT2 (Wickham, 2016) to visualize all phylogenetic trees presented in the current study (Figure 1b; Figures S1–S3). We report the log-combined trace file results for all BEAST runs in Table S4.

## 2.4 | Nuclear genome reconstruction, alignment and filtering

We selected two particularly well-preserved samples from Yukon for whole genome shotgun sequencing: YG303.325 and YG188.42, both dated to the Late Pleistocene (Table 1). For YG303.325, we extracted DNA from two ~0.12-g aliquots of bone powder and converted these extracts into six double-stranded, single-indexed DNA libraries (Kircher et al., 2012; Meyer & Kircher, 2010) that we then sequenced on dedicated lanes of an Illumina HiSeq-X ( $2 \times 150$  cycles) at the SciLifeLab (Stockholm, Sweden) and the HiSeq-2500

( $2 \times 100$  cycles) at the UC San Diego Institute for Genomic Medicine. For YG188.42 (YT03-40), we extracted DNA from three ~0.15-g aliquots of bone powder following the D1, D2, S1, S2, Y1 and Y2 methods (Gamba et al., 2016), and converted these extracts into nine double-stranded, single-indexed DNA libraries (Librado et al., 2017) which we sequenced at the Danish National DNA Sequencing Centre on dedicated lanes of the Illumina HiSeq-2500 instrument ( $1 \times 101$  cycles).

For both samples, we removed adapter sequences, merged paired-end reads that overlapped by at least 10 nucleotides, and removed reads shorter than 30 bp using SEQPREP2. We mapped retained reads (both merged and unmerged) to the horse reference genome assembly EquCab2.0 (GenBank: GCA\_000002305.1; Wade et al., 2009), using the BWA version 0.7.12 backtrack algorithm (Li & Durbin, 2009) with seed disabled as suggested by Schubert et al., (2012), converting SAM alignments into BAM alignments using BWA "sampe" for unmerged and "samse" for merged reads. We filtered out bases with a mapping quality <20 using SAMTOOLS version 0.1.19 (Li et al., 2009). We removed PCR (polymerase chain reaction)-duplicated reads using SAMTOOLS rmdup, and realigned reads around indels using the GATK version 3.7 indelrealigner (McKenna et al., 2010). We then explored patterns of DNA damage with MAPDAMAGE2 (Jónsson et al., 2013) and used this program to rescale quality scores taking into account the damage estimates, by using the --rescale and --fix-nicks flags (Figures S4–S6). We calculated genome-wide sequencing and type-specific error rates following Orlando et al., (2013) (Appendix S2, Table S5, Figure S7).

We added our two new palaeogenomes to a data set of seven previously published equid genomes (Table 1): Batagai (Librado et al., 2015); CGG10022 and CGG10023 (both Schubert et al., 2014); and Middle Pleistocene *E. cf. scotti* (TC21), present-day Przewalski's horse, Thoroughbred horse (Twilight) and *E. asinus* (donkey Willy; version mapped to horse) (all four from Orlando et al., 2013).

## 2.5 | Evaluating population structure

We detected population structure in our horse autosomal data set using ANGSD version 0.918 (Korneliussen et al., 2014) and genotype likelihoods (GLs) (Nielsen et al., 2011), which incorporate genotyping uncertainty that results from low coverage. We generated GLs for eight horses with ANGSD options -GL 2 -doGlf 2 -minQ 30 -minMapQ 30 -C 50 -rmTrans 1, and generated a GL covariance matrix with PCANGSD (Meisner & Albrechtsen, 2018). We used the R packages PRCOMP and FACTOEXTRA (Kassambara & Mundt, 2017) to run and visualize the principal component analysis (PCA) of the GL covariance matrix (Figure 2a).

## 2.6 | Estimating admixture

We ran an admixture analysis using the "-admix" flag in PCANGSD for  $K = 2$  to  $K = 5$  (Figure 2b; Figure S8), and visualized the results

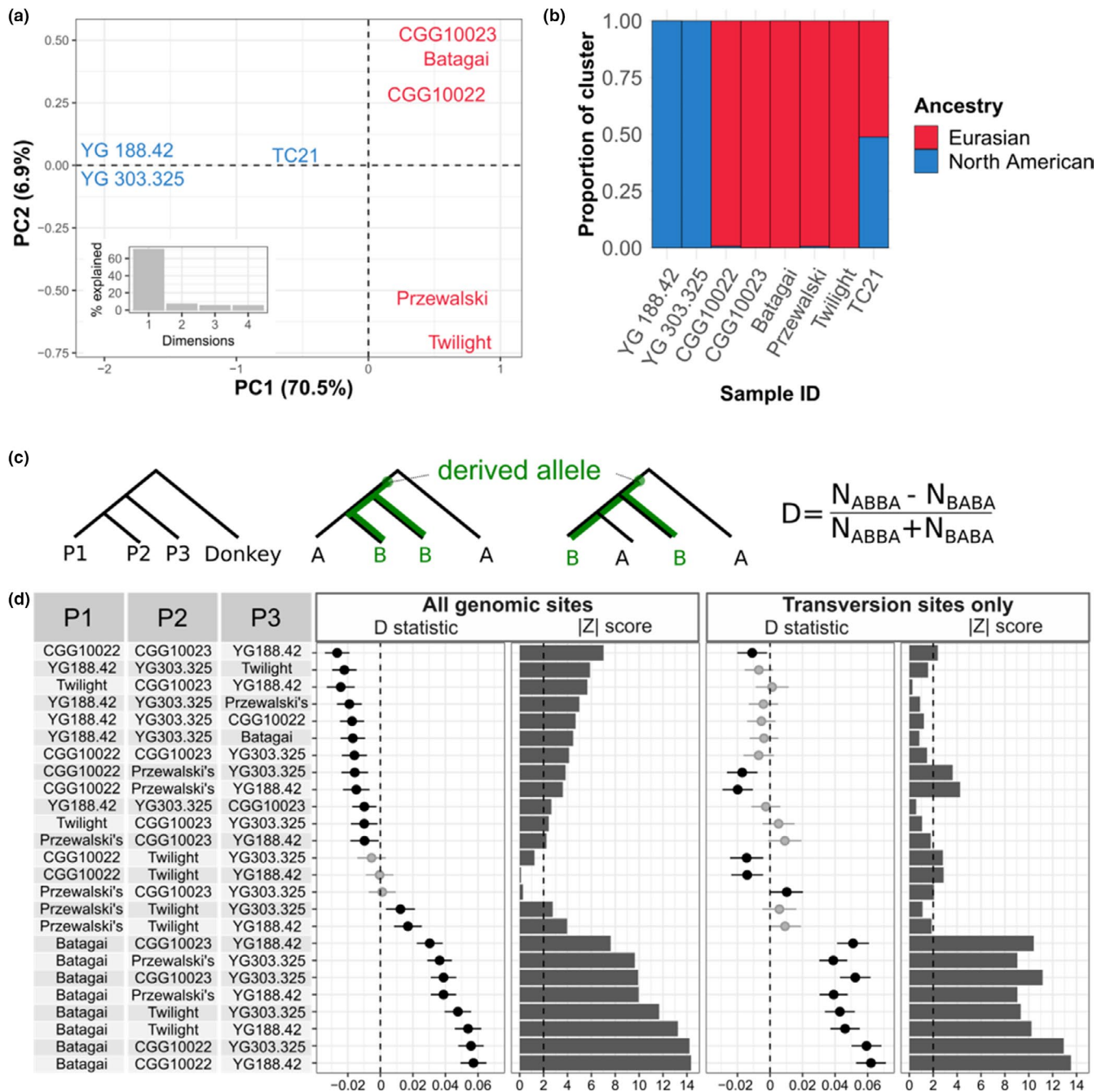


**FIGURE 2** Geographic structure and gene flow between present-day and ancient caballine horses. (a) Principal component (PC) analysis on the genotype likelihood covariance matrix. The percentage variation explained in the first four PCs is in the inset. (b) Admixture clustering for  $K = 2$ . Analyses for  $K = 3$  to  $K = 5$  are presented in Figure S5. Both (a) and (b) are estimated based on 6.7 million autosomal variable sites across eight horse genomes. In both (a) and (b) we excluded transitions to account for artefacts caused by post-mortem DNA damage. (c) Schematic of the D-statistic test for the patterns of derived allele sharing.  $D < 0$  suggests gene flow between P1 and P3, while  $D > 0$  suggests gene flow between P2 and P3. (d) D-statistic tests on all autosomal genomic sites (0.82 million ABBA+BABA sites on average per P1, P2 and P3 combination) and sites that exclude transitions (0.24 million ABBA+BABA sites on average per combination). Black and grey dots represent statistically significant and nonsignificant D-statistic values accordingly (estimated with Z-score using the jackknife.R script from the ANGSD package). We excluded the low-coverage TC21 horse from the D-statistic analysis. [Colour figure can be viewed at [wileyonlinelibrary.com](http://wileyonlinelibrary.com)]

with the R packages `RCPPCNPY` (Eddelbuettel & Wu, 2016) and `GGPLOT2` (Wickham, 2016). We next calculated D-statistics (ABBA/BABA test) using `ANGSD` to explore post-divergence admixture between sampled horse lineages (Durand et al., 2011; Green et al.,

2010). We excluded the Middle Pleistocene TC21 genome from this and all subsequent analyses due to its low coverage and age, which is close to the divergence of the caballine horse populations  $\sim 1.0$ – $0.8$  Ma. We polarized alleles using the donkey genome

and calculated the number of shared derived sites between one of the two closely related lineages (P1 and P2) and a possible introgressor (P3). As hybridization history can differ by sex (Cahill et al., 2015), we performed analyses separately for the autosomes and the X chromosome (Figure 2d; Figure S6). We used ANGSD “-doAbbababa 1” in 5-Mb chromosome blocks and computed the number of ABBA/BABA sites with ANGSD quality filters “-minQ 30 -minMapQ 30” and “-trim 5” to account for DNA damage at the ends of the reads and sequencing error rate difference between the genomes. Using this set of filters we ran D-statistic analysis on two data sets: with all genomic sites and with transition sites removed (Figure 2c,d). We considered the results to be significant if  $|Z| > 3$  and moderately significant if  $|Z| > 2$  (Barlow et al., 2018; Zheng & Janke, 2018) (Figure 2c,d; Figure S9).

To explore gene flow patterns further, we calculated the number of admixed nonoverlapping windows in our autosomal dataset using  $D_{FOIL}$  version 2017-011-25 (Pease & Hahn, 2015). The  $D_{FOIL}$  approach is similar to the D-statistic tests, but it expands the model to a five-population symmetric tree topology, which allowed us to test the directionality of gene flow. Following the phylogenetic position of the whole genome samples, we used Yukon horses as P1 and P2, Eurasian horses as P3 and P4, and donkey as an outgroup. We paired Eurasian samples only if they had close error rates to decrease the impact of false positive allele sharing (Appendix S2, Table S5; see Rasmussen et al., 2011). To run  $D_{FOIL}$ , we created pseudohaploid fasta files that excluded transitions to account for ancient DNA damage. To avoid reference bias, we called a random base at each site and filtered the data using the same criteria as the D-statistic analysis described above. We then split the genomes into 200-kb nonoverlapping windows with the BEDTOOLS makewindows tool. We converted each fasta file to  $D_{FOIL}$  counts and tested the treeness of a five-population model with native  $D_{FOIL}$  package scripts (Table S6, Figure S10).

## 2.7 | Estimating demographic history with G-PHOCS and PSMC

To infer demographic history and connectivity between horse populations in Eurasia and North America, we used the Bayesian coalescent approach implemented in G-PHOCS version 1.3 (Gronau et al., 2011), which reconstructs the coalescent process of multiple neutral loci assuming negligible recombination and selection. We excluded the low-coverage CCG10023 and TC21 horses and converted the base quality score recalibrated BAM alignments of other genomes to FASTA format using ANGSD “-doFasta 4 -doCounts 1 -minQ 25 -minMapQ 25 -uniqueOnly -setMinDepth 5 -setMaxDepth 100” (Korneliusson et al., 2014). We used the flag “-doFasta 4” in ANGSD to incorporate IUPAC ambiguity codes for variable sites, which allows G-PHOCS to iterate over all possible diploid phases (Gronau et al., 2011). To ascertain putatively neutral autosomal loci, we excluded sites with low and extremely high coverage, sites with low base quality, sites adjacent to indels, sites in clusters of apparent single

nucleotide polymorphisms (SNPs) or those in regions of the genome putatively undergoing selection as described below.

To gather coordinates of regions putatively affected by selection, we used annotations of the EquCab2 genome reference (Wade et al., 2009). We downloaded bed-files with exon data from Ensembl (Build 92) (Yates et al., 2020), tandem repeat tracks and genome assembly gaps from UCSC Genome Browser <http://genome.ucsc.edu/> (Karolchik et al., 2004), duplicated genes track from the Duplicated Genes database (Ouedraogo et al., 2012), simple and tandem repeats from the RepeatMasker database (Smit et al., 2013-2015), and coordinates of CpG islands from <http://www.haowulab.org/software/makeCGI/> (Irizarry et al., 2009; Wu et al., 2010).

To ascertain a high-quality set of variable sites (SNPs) among our genomes, we used BCFTOOLS version 1.1 (Li, 2011), ANTCALLER version 1.1 (Zhou et al., 2017) and GATK haplotypcaller to identify variants. We intersected the three call sets with VCFTOOLS version 0.1.16 vcf-isec (Danecek et al., 2011), and used only variants called by all three programs for downstream analysis. We filtered the final data set by removing SNPs with base call quality  $< 20$ , covered by fewer than five reads and located within 5 bp of indels. To limit the impact of multi-copy genes, we also removed SNPs with depth of coverage greater than the 0.995 quantiles of coverage distribution for each genome. Using BEDTOOLS, we created a “filter” file with genome coordinates for exons, genome assembly gaps, tandem and simple repeats, paralogues, CpG islands, and clustered SNPs (genomic intervals with two or more clustered SNPs within 5-, 10- and 50-bp windows), all of which we excluded from further analysis (see Figure S11 for the schematic). We extended each excluded region by 500 bp on both ends to account for selection and possible nearby genome misassemblies (Vitti et al., 2013). Using a custom python script, we ascertained a random set of 1-kb loci that would satisfy three criteria: (i) no overlap with the “filter” file coordinates; (ii) a minimum of 30-kb interlocus distance to avoid linkage disequilibrium; and (iii) a maximum of 10% missing nucleotides in each locus. This provided 4,215 putatively neutral 1-kb loci across all autosomes, separated by a median distance of 282 kb. To verify that the ascertained neutral loci data set followed the expected phylogenetic relationships between the samples, we concatenated all loci and used this alignment to reconstruct a phylogeny in GENEIOUS version 2020.0.5 (<https://www.geneious.com>) using the RAXML version 8.2.11 plugin (Stamatakis, 2014) (Figure S12).

We ran G-PHOCS on our ascertained data set of putatively neutral 1-kb loci. Since G-PHOCS is computationally intensive, we limited each run to only four samples: an outgroup (donkey) and one each of a present-day, ancient Eurasian and ancient North American horse genome (Figure 3a). This provided eight possible combinations. In each, we modelled three bidirectional migration bands, or intervals during which gene flow could have occurred between populations: m1 between ancestral North American and ancestral Eurasian populations; m2 between ancient North American and present-day horses; and m3 between ancient North American and ancient Eurasian populations. Migration bands are bounded by the time when the populations connected by gene flow existed; for example, the m1 migration



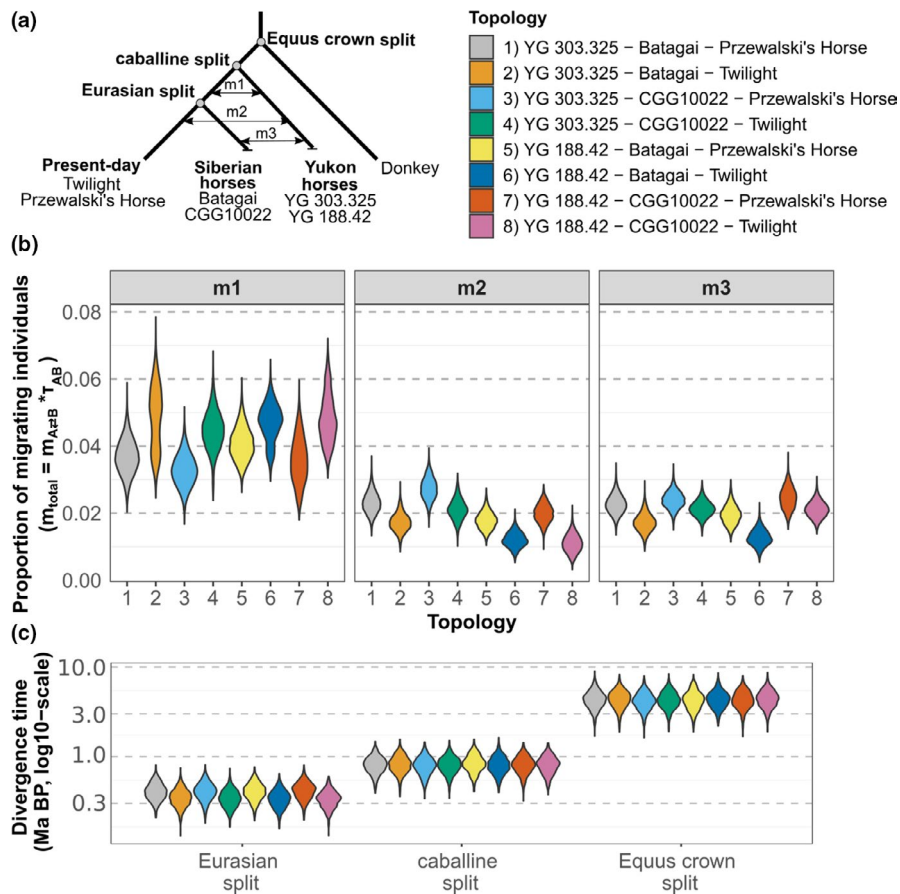


**FIGURE 3** Demographic history of caballine horses reconstructed with G-PHOCs. (a) A schematic of the tested demographic scenario. (b) Estimates of the migration rates. Since forward and backward migration rates were nearly identical, we collapsed their values when plotting the graph. (c) Divergence times. In the data set of 4,215 putatively neutral autosomal loci, there were 62,647 polymorphisms in the analysis with the donkey outgroup, including 26,627 sites segregating only in caballine horses. In each G-PHOCs run we used one genome per population (a), producing eight possible configurations of the tree topology as noted in the key. [Colour figure can be viewed at [wileyonlinelibrary.com](http://wileyonlinelibrary.com)]

band spans the entire time between  $T_{\text{North America-Eurasia divergence}}$  and  $T_{\text{Within Eurasia divergence}}$  (Figure 3a). We incorporated the following priors in the form of a gamma-distribution with the scale parameter  $\beta = 20,000$ : ages ( $\tau$ ) of the present-day samples were set to 0, ages of the ancient samples were set to their calibrated radiocarbon ages, the age of the root was set to the most recent common ancestor (MRCA) of *Equus* 4.5 Ma (Orlando et al., 2013), the MRCA of caballine horses was set to 1.0 Ma (Heintzman et al., 2017; Orlando et al., 2013), and the split between Eurasian populations was set to the younger boundary of 0.127 Ma, following Schubert et al., (2014). Posterior distributions of each parameter were recalculated to divergence times in units of years ( $T_{div}$ ) and effective population sizes ( $N_e$ ) by scaling with a per-generation mutation rate ( $\mu$ ) of  $7.24E-9$  and a generation time ( $g$ ) of 8 years (Orlando et al., 2013). We scaled the parameters using  $N_e = \theta/4\mu$ ,  $T_{div} = \tau g/\mu$ , where  $\theta$  is Watterson's estimator denoting population mutation rate (Figure S13).

The G-PHOCs migration band is modelled as a migration rate between two lineages over the time period when both of these lineages existed (Figure 3). Thus, we calculated the total migration rate  $m_{total}$  by scaling the per-generation migration rate  $m_{A \rightarrow B}$  by the duration of the corresponding migration bands  $\tau_{A \rightarrow B}$  (the length of the entire branch when both A and B populations existed). The  $m_{total}$  estimate is free of the assumption about the mutation rate (Gronau et al., 2011). Estimates of  $m_{total}$  approximate the probability that a locus sampled in a target population originated in the source population. To account for uncertainty in  $\mu$  and  $g$ , we randomly subsampled

these parameters from their gamma distributions while calibrating the G-PHOCs results: for  $\mu * E-9$  we used Gamma( $\alpha = 784, \lambda = 112$ ); for  $g$  - Gamma( $\alpha = 21, \lambda = 2.6$ ) (Figure S14).

We ran each model through the MCMC process three times to ensure a sufficient effective sampling size and parameter convergence, which we monitored in TRACER version 1.7.1 (Rambaut et al., 2018). We ran each MCMC chain for 10 million steps sampled every 10 iterations, removing the first 5% as burn-in, and allowed automatic fine-tuning of the parameters for the first 1,000 steps.

Next, we estimated changes in effective population size from each genome using the pairwise sequentially Markovian coalescent (PSMC) model (Li & Durbin, 2011). We generated a pseudohaploidized consensus sequence of the autosomes with SAMTOOLS MPILEUP using -EA options and -C50, followed by fq2psmcf -q20 (Li et al., 2009). We ran PSMC with parameters -N30 -t15 -r5 -p "4+25\*2+4+6" (Li & Durbin, 2011) (Figure S15).

### 3 | RESULTS

#### 3.1 | Mitochondrial and nuclear palaeogenomes of Pleistocene horses

We extracted ancient DNA from a total of 262 horse skeletal and dental remains, from which we selected 78 with sufficient preserved DNA for further processing. When reads were aligned to the

EquCab2 reference genome, all 78 libraries exhibited characteristic post-mortem ancient DNA damage and signal of depurination-driven DNA fragmentation: excesses of C > T and G > A transitions at the ends of the molecules, excess of purines in sites preceding read start positions, and short DNA fragment length (<100 bp) (Table S5, Figures S4–S5, S7). Using a combination of shotgun sequencing and hybridization-based enrichment, we assembled 19 new ancient Eurasian and 59 ancient North American horse mitochondrial genomes that ranged in coverage from 4.2- to 2,287-fold (median 22.8-fold) (Table S1), and two nuclear genomes of North American horses to an average coverage of 25.1- and 25.9-fold (Table 1; Figure S6). We complemented these data with previously published data to assemble a final data set of 190 mitochondrial and nine nuclear genomes (Figure 1a, Tables 1; S1 and S2). Below, we refer to horse populations on alternate sides of the BLB as “North American” or “Eurasian,” and to the ancient horse nuclear genomes by their geographically precise locations or by their museum catalogue numbers.

### 3.2 | Mitochondrial phylogeny of caballine horses

Horse mitochondrial genomes are strongly phylogeographically structured within Beringia, with two major clades corresponding to North America and Eurasia (Figure 1a,b; Figures S1–S3; Tables S1–S4), to which we assign clade designations following Weinstock et al., (2005). On the tip-calibrated BEAST analysis that included three outgroup sequences, we estimated that Clades A and B diverged 859–589 ka (95% highest posterior density [HPD]; median: 722 ka) (Figure S2, Table S4). This date is similar to that recovered with no outgroup (940–759 ka 95% HPD; median: 845 ka) and consistent with previous estimates (Heintzman et al., 2017; Orlando et al., 2013; Yuan et al., 2020). This timing coincides with the earliest of two dispersal events across the BLB identified in the CTMC model, which occurred around 875–625 ka in an east to west direction (Figure 1c).

We estimate a second dispersal across the BLB ~200–50 ka, predominantly in a west-to-east direction (Figure 1c). This signal is driven by two clusters of North American horses within clade A, which we designate A1 and A2 (Figure 1b). Clade A1 originated around 160–117 ka (95% HPD; median: 136 ka) and Clade A2 around 144–93 ka (95% HPD; median: 117 ka). Both clades A1 and A2 dispersed eastward at the same time, suggesting a single synchronous migration. Horses from clades A and B overlap geographically and temporally (Figure 1b; Figures S1–S3; Tables S1 and S2). Western Beringian horses of Clade B, in turn, are not monophyletic, in accordance with their maternal lineage redistribution during domestication (Fages et al., 2019; Gaunitz et al., 2018).

We found an unclear signal in the branching order of Clade C (Figure 1b). In our ML analysis, samples from present-day China, Russian Far East and New Siberian Islands (Clade C) cluster with Clade B, but with weak bootstrap support (61; see Figure S1). Previous studies, however, suggest the monophyly of Clade C with the Eurasian Clade A (Yuan et al., 2020). We found that rooting of the tree with outgroup sequences impacts the phylogenetic position

of this clade, in agreement with previously published results (Fages et al., 2019; Heintzman et al., 2017; Yuan et al., 2020). Thus, Clade C may represent a deeply divergent population of Eurasian caballine horses that have not been sampled sufficiently either in mtDNA or in whole genome data to resolve its polytomy at the root of the caballine horse tree.

### 3.3 | Population structure

The genetic relationships between present-day and ancient caballine horses reflect geography and time. On the PCA, the first principal component separates Eurasian and North American horses, while the second highlights variation between ancient and present-day Eurasian horses (Figure 2a). In the admixture analysis,  $K = 2$  separates samples into two groups corresponding to the present-day continental division between Eurasia and North America (Figure 2b; Figure S8). We found a small proportion of North American ancestry in CGG10022 (0.70%) and Przewalski's horses (0.65%). The early–Middle Pleistocene horse TC21, which lived close to the time of the initial divergence between Eurasian and North American horse populations, exhibits a mixed ancestry. Consistent with the antiquity of its genome, it falls between all other sampled individuals in both analyses (Figure 1b; Orlando et al., 2013).

### 3.4 | D-statistic and $D_{FOIL}$

We found a significant excess of alleles shared among ancient Siberian, ancient Yukon, and present-day horses with the D-statistic test and  $D_{FOIL}$  analysis (Figure 2c,d; Figure S8). Out of 11,225 200-kb nonoverlapping genomic windows, ~10% ( $n = 1,156$ ) were admixed between Yukon, YG188.42 and YG303.325, and ancient Taymyr, CGG10022 and CGG10023 (Table S6, Figure S10). For the Batagai, Przewalski's and Twilight horses we found ~7.7% admixed windows ( $n = 869.7$  on average across three  $D_{FOIL}$  tests) (Figure S10, Table S6). We observed similar allele sharing patterns on both autosomes and the X-chromosome regardless of whether nucleotide transitions, which are more strongly impacted by post-mortem DNA damage, were included or excluded (Figure 2d; Figure S9). For each five-population topology tested with  $D_{FOIL}$ , we found bidirectional gene flow between Yukon genomes and either of the Eurasian individuals (Figure S10).

We found a contradictory pattern of gene flow between Batagai and Yukon horses. In the D-statistic test, Batagai does not have a statistically significant excess of allele sharing with either of the North American horses (Figure 2d). However, in the  $D_{FOIL}$  analysis, we found 7%–8% of genomic windows admixed between Batagai and Yukon horses in either direction (Table S6, Figure S10). We note that the sequencing error rate in the Batagai genome is lower than error rates in CGG10022 and CGG10023 (Appendix S2, Table S5), which can inflate sensitivity of the D-statistic when these genomes are tested as P1 and P2, but not as P3 (Rasmussen et al., 2011).

Nevertheless, in the D-statistic analysis, Batagai did not share excess alleles with either of the Yukon horses when tested as P3 or with a present-day horse when tested as P1. For the  $D_{\text{FOIL}}$  analysis, we only tested Batagai with present-day Eurasian horses that had similar error rates (Figure S10). Batagai's contradictory admixture pattern held regardless of the four- and five-taxon test configuration.

### 3.5 | Gene flow and demographic history

To further explore the timing and extent of admixture between Eurasian and North American horse populations, we fitted a demographic model using G-PHOCs (Figure 3a,b,c; Figure S13) (Gronau et al., 2011). We estimated the total migration rate within three bidirectional migration bands connecting horse lineages corresponding to mitochondrial clades A and B (denoted m1–3, Figure 3a,b), as well as the divergence time among them (Figure 3c). Assuming a mutation rate centred around  $7.242\text{E-}9$  per site per generation (Orlando et al., 2013), caballine horses diverged from their sister species *E. asinus*  $4.4 \pm 1$  Ma (Figure 3c). Eurasian and North American caballine horse populations diverged  $0.818 \pm 0.187$  Ma, which is slightly younger than a previous estimate of 1.062 Ma (Orlando et al., 2013) but consistent with the 1.0–0.7 Ma estimate of their mitochondrial divergence (Heintzman et al., 2017) and our time-calibrated mitochondrial phylogeny (Figure 1b). In analyses in which the Przewalski's horse was in the position of the present-day population, we estimated a slightly older divergence between the ancestors of extinct and present-day Eurasian caballine horses ( $416 \pm 0.9$  ka) compared to  $346 \pm 0.8$  ka with the Twilight horse in this position (note that these estimates do not account for post-divergence gene flow between extinct Eurasian horses and the ancestors of domestic horses). These estimates are similar to the estimate of 384 ka BP from Schubert et al., (2014), but younger than an estimate of ~625–500 ka (Orlando et al., 2013) that included the Middle Pleistocene TC21 genome. Because lineages diverge gradually in the presence of gene flow, these estimates represent upper boundaries (Edwards & Beerli, 2000).

During the period that followed the initial divergence between Eurasian and North American populations (m1), we estimated a total migration rate of  $4.0 \pm 0.8\%$  across the BLB (Figure 3b). The total migration rate is determined by multiplying the number of migrants per generation with the time span of the migration band, which in this case corresponds to 3%–4% migration probability during the Middle Pleistocene. After this initial divergence, the migration rate declined to ~2%. While the migration rate in all three bands differs from zero, we do not have statistical power given our sample size to determine directionality. Finally, in contrast to the D-statistic tests but similar to the  $D_{\text{FOIL}}$  result, the Batagai genome displays signatures of gene flow from either of the Yukon horses.

G-PHOCs estimates suggest that the effective population size ( $N_e$ ) of the North American horse population was smaller than that of the Pleistocene Taymyr horses ( $N_e \approx 30,000$ – $32,000$  and  $N_e \approx 48,000$ , accordingly, Figures S13). This smaller  $N_e$  is also reflected in PSMC plots from each horse (Figure S15). The estimated  $N_e$  for the

~5.5-ka-old Batagai horse is  $\approx 18,000$ , which is consistent with the sharp decline in its PSMC profile beginning ~10,000 years prior to its death (Figure S15) and previous reports of a predomestication bottleneck (Librado et al., 2015). Estimates of  $N_e$  are similar for the Przewalski ( $N_e \approx 19,000$ ) and Thoroughbred ( $N_e \approx 18,000$ ) horses.

## 4 | DISCUSSION

Although the BLB was a barrier for dispersal for much of the last million years of horse evolutionary history, horses used the land bridge when it was viable. Caballine horse populations on the two sides of the corridor maintained low levels of gene flow and biological connectivity until at least the time of the Last Glacial Maximum (LGM), 26–20 ka (Figure 4). Signatures of bidirectional dispersal across the BLB are present in both our mitochondrial and nuclear data sets. The latter provided an estimate of continuous gene flow equivalent to 2%–4% of the population migrating across the BLB during the Pleistocene and ~0.6%–0.7% of North American ancestry in ancient and present-day horses in Eurasia (Figures 2b,c and 3b; S9 and S10). This suggests that caballine horses in Beringia functioned as a metapopulation, at least until the local extinction of horses in North America and flooding of the BLB in the early Holocene (Figure 4).

Our mitochondrial phylogeny reveals at least two intercontinental dispersal events across the BLB during the Pleistocene (Figures 1 and 4). The first, which we estimate to have been predominantly in the east-to-west direction, occurred between ~0.95 and ~0.45 Ma (Figures 1c and 4). The start of the dispersal event is consistent with the age of the earliest recognized caballine horses in Eurasia ~0.9–0.8 Ma (Azzaroli, 1983, 1989; Forsten, 1996), and therefore may reflect the first wave of caballine horse dispersal into Eurasia from North America. The second dispersal occurred between ~0.2 and ~0.05 Ma, a time interval corresponding to an open BLB during the lowered sea level associated with MIS 6 glaciation. This second dispersal was bidirectional but dominated by west-to-east movement from Eurasia into North America. Horses dispersing into North America during this interval migrated east as far as Alaska's North Slope and Northern Yukon, where members of the Eurasian-origin Clade A1 co-occur temporally with the established North American Clade B, providing opportunity for horses of these two mitochondrial lineages to interbreed.

The temporal windows identified in the mitochondrial phylogeny coincide with periods when the BLB would have been open and available to dispersing megafauna, but are otherwise limited by our sampling (few samples from Middle and early–Late Pleistocene, and no North American samples that lived more recently than ~13 ka BP). Our data may therefore fail to capture other intervals during which horses could have dispersed across the BLB (e.g., between ~800 and 50 ka, and after 13 ka). Geological and palaeoclimatic data indicate that the BLB was flooded after ~13 ka (Elias et al., 1996; England & Furze, 2008; Hu et al., 2012) and perhaps as late as ~11 ka (Jakobsson et al., 2017), which would have provided opportunity for gene flow until the early Holocene. Data from the Middle

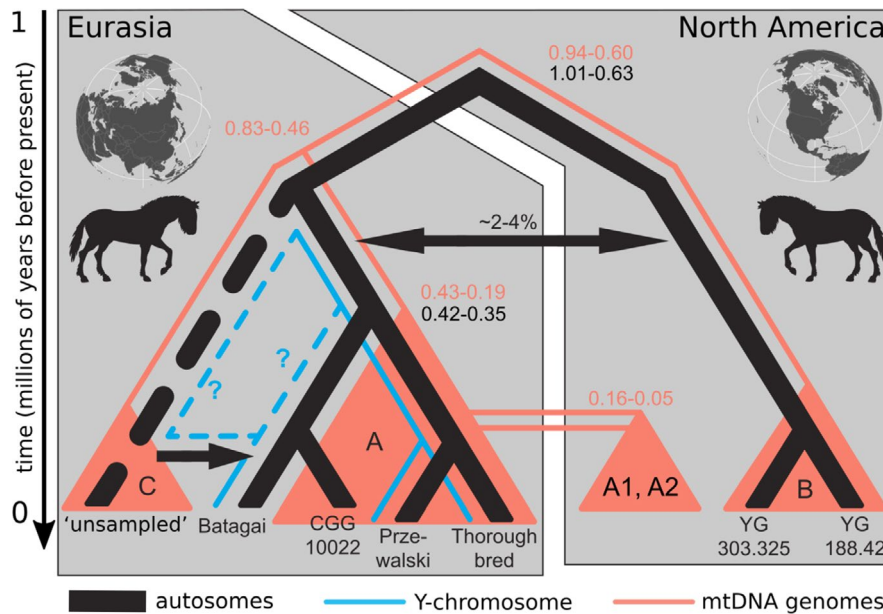


**FIGURE 4** A tentative demographic scenario of caballine horse evolution. The Eurasian caballine horses (mitochondrial clades A and C) diverged from North American caballines (clade B) ~1.0–0.8 Ma via dispersal across the Bering Land Bridge (BLB). The evolution of horses continued on both continents in the presence of gene flow across the BLB. Cold conditions during the Middle Pleistocene and MIS 6 openings of the BLB facilitated local dispersals, leading to cross-continental migration of Eurasian horses back to North America (clades A1, A2). Many extinct lineages of horses are still undersampled (Librado & Orlando, 2020; Orlando, 2020), including an as yet unsampled population that diverged from other Eurasian horses prior to substantial gene flow between Eurasian and North American horses. We assume that this population with unsampled nuclear genome ancestry belongs to the divergent mitochondrial Clade C. We further hypothesize that this unsampled population contributed to the ancestry of the Batagai horse based on our D-statistic and  $D_{FOIL}$  results. This hypothesis may be further supported by the phylogenetic signal of Batagai's uniparental loci (Fages et al., 2019). All North American horses (clades A1, A2, B) and Clade C went extinct by the early Holocene ~11 ka. Divergence times for mtDNA genomes are from the BEAST analyses, whereas those for the autosomes are from the G-PHOCs analyses. Arrows represent gene flow, as inferred by admixture analysis, D-statistics,  $D_{FOIL}$  and G-PHOCs. Horse silhouettes are from phylogenic.org; image by M. Yrayzoz (vectorized by T. Michael Keesey and reused under a CC-BY-3.0 licence). No changes were made other than vertically flipping the image on the left). Globes are plotted in R with RWORLDMAP (South, 2011; Wickham, 2016) [Colour figure can be viewed at wileyonlinelibrary.com]

Pleistocene and late surviving North American horses may reveal additional dispersal events across the BLB.

Although mitochondrial data can only identify dispersal events across the BLB, our nuclear genomic analyses confirm that dispersal events led to bidirectional gene flow between horse populations in Eurasia and North America (Figures 2b,c,d, 3a,b and 4; Table S6, Figure S10). Immediately following the initial colonization of Eurasia by horses ~0.8 Ma, gene flow between the continents was maintained at a rate of around 3%–4%. This migration rate declined after the Middle Pleistocene to around 2%, suggesting that, while gene flow was maintained across the BLB until at least the LGM, relatively fewer individuals were dispersing, or fewer dispersing individuals were integrating into local populations, during the Late Pleistocene (Figure 3c). The decline may be due in part to decreasing availability of the BLB during ~130–60 ka, and perhaps as late as 40 ka, as the Bering Sea level hovers close to the transgression depth at that time (Hu et al., 2010, 2012). This higher sea level may have enhanced an ecological barrier between western and eastern Beringia if the Mammoth Steppe was less permeable (e.g., Guthrie, 2001). Other factors also may have contributed to the overall reduction in gene flow, such as challenges to immigrants integrating into established

populations, as yet unknown ecological barriers limiting local dispersals, or postzygotic isolation (Coughlan & Matute, 2020; Orr et al., 2004; Orr & Presgraves, 2000; Savolainen et al., 2013; Turelli & Orr, 2000). Teasing apart the relative roles of these processes will require denser sampling of horses from across Eastern Beringia.

The decline in gene flow over time is also supported by D-statistic tests (Figures 2c,d; S9). CGG10022 is dated to ~43 ka BP, and appears to be the most admixed in the panel. CGG10023, which is dated to ~16 ka BP, shares fewer alleles than the older Siberian horse does with either Yukon horse, and the ~5 ka BP Batagai horse does not appear to share an excess of derived alleles with either of the Yukon horses (Figure 2b,c). The decreasing admixture signal may be due to selection against North American ancestry, perhaps similar to observed selection against deleterious Neanderthal alleles in humans (Juric et al., 2016), or may result from subsequent gene flow with an unsampled lineage without North American ancestry (Figure 4). While we prefer the latter explanation, given that Western and Eastern Beringian horses were adapted to such similar environments, additional genomic data will be necessary to test these alternative hypotheses. Whole genome data, such as high-coverage genomes or targeted enrichment of ancestry-informative

SNPs, from clade A1 and A2 horses has the potential to provide additional insight into gene flow patterns between Western and Eastern Beringian horses.

Additional horse genomes will also continue to refine understanding of how genetic diversity was partitioned within continental populations. For example, we found evidence that an as-yet unsampled horse population contributed ancestry to the Batagai horse (Figures 2c, 3b and 4). While we observed post-divergence gene flow between the Siberian, domestic and Yukon horses, D-statistics did not indicate shared ancestry between Batagai and either Yukon horse. However,  $G\text{-PHOCS}$  and  $D_{\text{FOIL}}$  suggested gene flow across the BLB when Batagai was included (Figure 3b). These contrasting patterns may be due to ancestral population structure within Eurasia. Thereby, North American horses contributed alleles into some populations but not others, and an as yet unsampled Eurasian population contributed ancestry into the Batagai genome but not to the more ancient horse from Taymyr (Figure 4). Possibly supporting this hypothesis, a previous study suggested that an as yet unsampled population contributed ancestry to some ancient Siberian horse populations (Fages et al., 2019; Orlando, 2020). The evolutionary history of uniparental markers differs in Eurasian horses, with Batagai falling either within (per mtDNA) or outside (per Y-chromosome) the diversity of other Eurasian horses analysed here (Fages et al., 2019), further hinting at an unsampled source of ancestry. A potential candidate for this population with unclear nuclear genome ancestry is the East Asian mitochondrial Clade C (Figures 1b and 4), assigned the name *Equus dalianensis* by Yuan et al., (2020). *E. dalianensis* had a range that extended westward to the region of present-day Kazakhstan, the putative centre of horse domestication (Librado & Orlando, 2020; Orlando, 2020), and northward to Chukotka, where the Batagai horse was recovered (Librado et al., 2015), but not as far northward as Taymyr, where CGG10022 was found (Orlando et al., 2013). Although additional genetic data from *E. dalianensis* will be necessary to test this hypothesis directly, our results suggest a more complex model of horse population structure and dispersals than is reflected in existing data. While the maternally inherited nonrecombining mitochondrial locus provides limited information, nuclear genome data enable direct estimates of gene flow and population isolation in cases of complex evolutionary histories, such as those of caballine horses. Thus, whole-genome sequencing of even a few samples is a more promising approach for resolving this question.

Our results have implications for horse taxonomy and palaeontology. We observed that present-day Przewalski's and domestic horses have a proportion of genomic ancestry that derives from relatively recent gene flow from extinct North American horses. From a systematic perspective, fossils of Late Quaternary caballine equids from Western and Eastern Beringia have been attributed on morphological grounds to a variety of nominally separate species, including *Equus ferus*, *E. lambei*, *E. alaskae*, *E. lenensis*, *E. dalianensis* and *E. scotti* among many others (Azzaroli, 1989; Azzaroli & Voorhies, 1993; Barron-Ortiz et al., 2019; Barrón-Ortiz et al., 2017). Some of these are surely *nomina nuda* (empty names), with no real standing in biology even if their nomenclature is correctly formed.

Although recent genomic investigations have shown that evolutionary diversification has occurred in caballine populations during the Pleistocene (e.g., Weinstock et al., 2005; Barrón-Ortiz et al., 2017; Heintzman et al., 2017), the number of lineages sufficiently distinct to warrant formal taxonomic recognition is small. In the case of the Pleistocene Beringian caballines considered here, it is reasonable to view them as a bicontinental metapopulation, component parts of which were in intermittent biological contact via the BLB. How this should be reflected systematically is, however, not straightforward. For example, although complete reproductive isolation of caballines on opposite sides of the Bering Strait was evidently never achieved, the comparatively low hybridization rate detected in our samples indicates that metapopulation mixing was limited even when the BLB was available. Thus, a different method of discriminating population boundaries is needed.

One way of recognizing continuities as well as differences among closely related populations within a widely distributed species is to distinguish subspecies. Ideally, formally defined subspecies ought to have congruent phenotypic and genotypic identities and live in circumscribed geographical spaces, so that they can be distinguished from other clusters from which they are spatially, but not reproductively, isolated (Patten, 2015). This is a hard standard to meet when dealing with fossil populations, which can only be partially characterized for these parameters. Indeed, because of the blurring effects of convergence and hybridization within *E. ferus*, the only generally recognized horse subspecies is extant *E. f. przewalskii*, previously considered a different species (Gaunitz et al., 2018). As Barrón-Ortiz et al., (2017) have pointed out, efforts to distinguish extinct populations of *E. ferus* from the Western Interior of North America as subspecies (e.g., *E. f. lambei*, *E. f. scotti*) does not clarify their evolutionary position because morphological and mtDNA analysis of these otherwise distinct populations demonstrates their extensive similarities. Furthermore, Eurasian populations of *Equus* sp. have markedly different evolutionary histories when their mitochondrial, Y-chromosome and autosomal phylogenies are compared (Fages et al., 2019; this study, Figure 4). Defining populations using individual and/or uniparentally inherited genetic markers is as equally challenging as using size-related morphological differences as a basis for taxonomic classification (see Saarinen et al., 2021). Such manoeuvres may be theoretically justifiable, but, in the case of caballine horses, risk providing little insight into this taxon's true evolutionary history and systematic status. Until a strong basis for formalizing biological distinctions among Quaternary Holarctic caballine horses can be established, it is preferable to avoid formal trinomials or similar devices, and to refer instead to "Eurasian clades" and "North American clades" as we have done here.

Finally, our study demonstrates the advantage of genomics in identifying the role of the BLB not only as a biogeographical corridor, but also as a critical contact zone where significant evolutionary processes unfolded for Holarctic cold adapted taxa (Figure 4). Our data show that horses dispersed back into North America from Eurasia around the same time as the initial expansion of bison, brown bears

and lions through the BLB (Froese et al., 2017; Salis et al., 2020). When present, the BLB clearly played a key role as a bicontinental dispersal corridor for many taxa, including ones that used it more than once (Debruyne et al., 2008; Elias & Crocker, 2008; Froese et al., 2017; Meiri et al., 2014, 2020). This Ice Age fauna thrived on the Mammoth Steppe, the widespread steppe–tundra biome present in Beringia during cold periods of the Pleistocene (Guthrie, 1982; Zimov et al., 2012). With the onset of dramatic climate change and ultimate disappearance of the BLB at the end of the Pleistocene, the biogeographical importance of this ecological corridor fundamentally changed for terrestrial taxa.

## ACKNOWLEDGMENTS

We are grateful to the placer gold mining community, the Tr'ondëk Hwëch'in First Nation, and the Vuntut Gwitchin First Nation for their collaboration and support with our research in Yukon. Tamara Pico, Sarah Crump and Paul Koch provided advice interpreting the palaeoclimate of Beringia. Data generation was supported with funds from NSF ARC-1417036, the Gordon & Betty Moore Foundation (no. 3804) and the American Wild Horse Campaign. A.O.V. was additionally supported by a UCSC Chancellor's Dissertation Year Fellowship and the CANA Foundation. M.T. and D.G. were supported by the Russian Foundation for Basic Research (project 18-04-00327), and L.E. by a Marie-Curie Intra-European fellowship (FP7, IEF-302617). G.B. is supported by the Federal theme of Zoological Institute of the Russian Academy of Sciences no. AAAA-A19-119032590102-7. S.V. was funded by the Russian Foundation for Basic Research, Grant 19-05-00477. L.D. acknowledges support from FORMAS (project 2018-01640). D.F. was supported by the Natural Science and Engineering Research Council. P.G. and D.M. are supported by the Bureau of Land Management. We acknowledge support from Science for Life Laboratory, the Knut and Alice Wallenberg Foundation, the National Genomics Infrastructure funded by the Swedish Research Council, and Uppsala Multidisciplinary Center for Advanced Computational Science for assistance with massively parallel sequencing and access to the UPPMAX computational infrastructure. L.O. received funding from the European Research Council (ERC) under the European Union's Horizon 2020 research and innovation programme (grant agreement 681605).

## AUTHOR CONTRIBUTIONS

B.S., P.G., D.H.M., L.O. and R.D.M. conceived the study. P.G., D.H.M., B.S., G.Z., G.B., D.G., E.H., S.H., I.K., P.K., F.S., H.T., M.T., E.S., S.V. and L.D. performed field work and provided the samples. A.O.V., P.D.H., M.C.J., C.D.S., S.G.D., L.E., L.D., C.G., J.D.K., A.S.O. and M.S. generated data. J.S. generated radiocarbon data. A.O.V. and P.D.H. analysed the data with contributions from R.C.D., B.S. and L.O. B.S., R.D.M., A.O.V., P.D.H., R.C.D., G.Z., D.F., P.G., D.M. and L.O. interpreted the data. A.O.V. wrote the initial manuscript draft. B.S., R.D.M. and P.D.H. revised the manuscript with A.O.V., with contributions from L.O., D.F., R.C.D., G.Z., P.G., D.H.M., M.J.W. and I.K.

## DATA AVAILABILITY STATEMENT

Radiocarbon dates have been uploaded to the Arctic Data Center (<https://doi.org/10.18739/A28C9R40R>). Raw sequencing data generated from YG303.325 and YG188.42 are available in NCBI BioProject PRJNA727160 (SAMN19007726, SAMN19007727). All newly generated mitochondrial genomes have been uploaded to GenBank with ID nos. MW846090–MW846167. BEAST files and the final G-PHOCS “filter” file are available on Data Dryad <https://doi.org/10.7291/D18W9G>. All scripts, as well as filtering criteria used to ascertain the set of putatively neutral loci, are published on github [https://github.com/avershinina/BLB\\_horses](https://github.com/avershinina/BLB_horses).

## ORCID

Alisa O. Vershinina  <https://orcid.org/0000-0002-3120-6592>  
 Peter D. Heintzman  <https://orcid.org/0000-0002-6449-0219>  
 Love Dalén  <https://orcid.org/0000-0001-6307-8188>  
 Luca Ermini  <https://orcid.org/0000-0001-8109-6021>  
 Ludovic Orlando  <https://orcid.org/0000-0003-3936-1850>  
 Beth Shapiro  <https://orcid.org/0000-0002-2733-7776>

## REFERENCES

- Alter, S. E., Meyer, M., Post, K., Czechowski, P., Gravlund, P., Gaines, C., Rosenbaum, H. C., Kaschner, K., Turvey, S. T., van der Plicht, J., Shapiro, B., & Hofreiter, M. (2015). Climate impacts on transoceanic dispersal and habitat in gray whales from the Pleistocene to 2100. *Molecular Ecology*, 24(7), 1510–1522.
- Azzaroli, A. (1983). Quaternary mammals and the “end-Villafranchian” dispersal event—a turning point in the history of Eurasia. *Palaeogeography, Palaeoclimatology, Palaeoecology*, 44(1–2), 117–139.
- Azzaroli, A. (1989). The Genus *Equus* in Europe. In E. H. Lindsay, V. Fahlbusch, & P. Mein (Eds.), *European Neogene Mammal Chronology* (pp. 339–356). Springer, US.
- Azzaroli, A., & Voorhies, M. R. (1993). The genus *Equus* in North America. The Blancan species. *Palaeontographia Italica*, 80, 175–198.
- Barlow, A., Cahill, J. A., Hartmann, S., Theunert, C., Xenikoudakis, G., Fortes, G. G., Pajmans, J. L. A., Rabeder, G., Frischauf, C., Grandal-d'Anglade, A., García-Vázquez, A., Murtskhvaladze, M., Saarma, U., Anijalg, P., Skrbinšek, T., Bertorelle, G., Gasparian, B., Bar-Oz, G., Pinhasi, R., ... Hofreiter, M. (2018). Partial genomic survival of cave bears in living brown bears. *Nature Ecology & Evolution*, 2(10), 1563–1570.
- Barron-Ortiz, C., Avilla, L., Jass, C., Bravo-Cuevas, V., Machado, H., & Mothé, D. (2019). What is *Equus*? Reconciling taxonomy and phylogenetic analyses. *Frontiers in Ecology and Evolution*, 7, 343.
- Barrón-Ortiz, C. I., Rodrigues, A. T., Theodor, J. M., Kooyman, B. P., Yang, D. Y., & Speller, C. F. (2017). Cheek tooth morphology and ancient mitochondrial DNA of late Pleistocene horses from the western interior of North America: Implications for the taxonomy of North American Late Pleistocene *Equus*. *PLoS One*, 12(8), e0183045.
- Bond, J. D. (2019). *Paleodrainage map of Beringia*. Retrieved November 20, 2020, from Yukon Geological Survey website: <http://data.geology.gov.yk.ca/Reference/81642#InfoTab>
- Cahill, J. A., Stirling, I., Kistler, L., Salamzade, R., Ersmark, E., Fulton, T. L., Stiller, M., Green, R. E., & Shapiro, B. (2015). Genomic evidence of geographically widespread effect of gene flow from polar bears into brown bears. *Molecular Ecology*, 24(6), 1205–1217.
- Chang, D., Knapp, M., Enk, J., Lippold, S., Kircher, M., Lister, A., A., MacPhee, R. D. E., Widga, C., Czechowski, P., Sommer, R.,

- Hodges, E., Stümpel, N., Barnes, I., Dalén, L., Derevianko, A., Germonpré, M., Hillebrand-Voiculescu, A., Constantin, S., ... Shapiro, B. (2017). The evolutionary and phylogeographic history of woolly mammoths: a comprehensive mitogenomic analysis. *Scientific Reports*, 7, 44585.
- Coughlan, J. M., & Matute, D. R. (2020). The importance of intrinsic postzygotic barriers throughout the speciation process. *Philosophical Transactions of the Royal Society of London. Series B, Biological Sciences*, 375(1806), 20190533.
- Coyne, J. A., & Orr, H. A. (1998). The evolutionary genetics of speciation. *Philosophical Transactions of the Royal Society of London. Series B: Biological Sciences*, 353(1366), 287–305.
- Dabney, J., & Meyer, M. (2019). Extraction of Highly Degraded DNA from Ancient Bones and Teeth. In B. Shapiro, A. Barlow, P. D. Heintzman, M. Hofreiter, J. L. A. Paijmans, & A. E. R. Soares (Eds.), *Ancient DNA: Methods and Protocols* (pp. 25–29). Springer New York.
- Danecek, P., Auton, A., Abecasis, G., Albers, C. A., Banks, E., DePristo, M. A., Handsaker, R. E., Lunter, G., Marth, G. T., Sherry, S. T., McVean, G., & Durbin, R., 1000 Genomes Project Analysis Group (2011). The variant call format and VCFtools. *Bioinformatics*, 27(15), 2156–2158.
- Darriba, D., Taboada, G. L., Doallo, R., & Posada, D. (2012). jModelTest 2: more models, new heuristics and parallel computing. *Nature Methods*, 9(8), 772.
- Debruyne, R., Chu, G., King, C. E., Bos, K., Kuch, M., Schwarz, C., Zazula, G., Guthrie, D., Froese, D., Buigues, B., Marliave, C., Flemming, C., Poinar, D., Fisher, D., Southon, J., Tikhonov, A. N., MacPhee, R. D. E., & Poinar, H. N. (2008). Out of America: ancient DNA evidence for a new world origin of late quaternary woolly mammoths. *Current Biology: CB*, 18(17), 1320–1326.
- Durand, E. Y., Patterson, N., Reich, D., & Slatkin, M. (2011). Testing for ancient admixture between closely related populations. *Molecular Biology and Evolution*, 28(8), 2239–2252.
- Dyke, A. S. (2004). An outline of North American deglaciation with emphasis on central and northern Canada. *Quaternary Glaciations-Extent and Chronology - Part II: North America*, 2, 373–424. [https://doi.org/10.1016/s1571-0866\(04\)80209-4](https://doi.org/10.1016/s1571-0866(04)80209-4)
- Eddelbuettel, D., & Wu, W. (2016). RcppNPY: Read-write support for NumPy files in R. *Journal of Open Source Software*, 1(5), 55.
- Edgar, R. C. (2004). MUSCLE: multiple sequence alignment with high accuracy and high throughput. *Nucleic Acids Research*, 32(5), 1792–1797.
- Edwards, S. V., & Beerli, P. (2000). Perspective: gene divergence, population divergence, and the variance in coalescence time in phylogeographic studies. *Evolution*, 54(6), 1839–1854.
- Elias, S. A., & Brigham-Grette, J. (2013). Late Pleistocene Glacial Events in Beringia. In S. A. Elias, & C. J. Mock (Eds.), *Encyclopedia of Quaternary Science*, 2nd ed. (pp. 191–201). Elsevier.
- Elias, S. A., & Crocker, B. (2008). The Bering Land Bridge: a moisture barrier to the dispersal of steppe-tundra biota? *Quaternary Science Reviews*, 27(27), 2473–2483.
- Elias, S. A., Short, S. K., Hans Nelson, C., & Birks, H. H. (1996). Life and times of the Bering land bridge. *Nature*, 382, 60–63. <https://doi.org/10.1038/382060a0>.
- England, J. H., & Furze, M. F. A. (2008). New evidence from the western Canadian Arctic Archipelago for the resubmergence of Bering Strait. *Quaternary Research*, 70(1), 60–67.
- Fages, A., Hanghøj, K., Khan, N., Gaunitz, C., Seguin-Orlando, A., Leonardi, M., McCrory Constantz, C., Gamba, C., Al-Rasheid, K. A. S., Albizuri, S., Alfarhan, A. H., Allentoft, M., Alquraishi, S., Anthony, D., Baimukhanov, N., Barrett, J. H., Bayarsaikhan, J., Benecke, N., Bernáldez-Sánchez, E., ... Orlando, L. (2019). Tracking five millennia of horse management with extensive ancient genome time series. *Cell*, 177(6), 1419–1435.e31.
- Forstén, A. (1991). Mitochondrial-DNA time-table and the evolution of Equus: comparison of molecular and paleontological evidence. *Annales Zoologici Fennici*, 28(3/4), 301–309.
- Forsten, A. (1996). Climate and the evolution of Equus [Perissodactyla, Equidae] in the Plio-Pleistocene of Eurasia. *Acta Zoologica Cracoviensia*, 1(39), 161–166.
- Froese, D., Stiller, M., Heintzman, P. D., Reyes, A. V., Zazula, G. D., Soares, A. E. R., Meyer, M., Hall, E., Jensen, B. J. L., Arnold, L. J., MacPhee, R. D. E., & Shapiro, B. (2017). Fossil and genomic evidence constrains the timing of bison arrival in North America. *Proceedings of the National Academy of Sciences of the United States of America*, 114(13), 3457–3462.
- Fulton, T. L., & Shapiro, B. (2019). Setting Up an Ancient DNA Laboratory. In B. Shapiro, A. Barlow, P. D. Heintzman, M. Hofreiter, J. L. A. Paijmans, & A. E. R. Soares (Eds.), *Ancient DNA: Methods and Protocols* (pp. 1–13). Springer New York.
- Gamba, C., Hanghøj, K., Gaunitz, C., Alfarhan, A. H., Alquraishi, S. A., Al-Rasheid, K. A. S., Bradley, D. G., & Orlando, L. (2016). Comparing the performance of three ancient DNA extraction methods for high-throughput sequencing. *Molecular Ecology Resources*, 16(2), 459–469.
- Gaunitz, C., Fages, A., Hanghøj, K., Albrechtsen, A., Khan, N., Schubert, M., Seguin-Orlando, A., Owens, I. J., Felkel, S., Bignon-Lau, O., Damgaard, P. B., Mittnik, A., Mohaseb, A. F., Davoudi, H., Alquraishi, S., Alfarhan, A. H., Al-Rasheid, K. A. S., Crubézy, E., Benecke, N., ... Orlando, L. (2018). Ancient genomes revisit the ancestry of domestic and Przewalski's horses. *Science*, 360(6384), 111–114.
- Gill, M. S., Lemey, P., Faria, N. R., Rambaut, A., Shapiro, B., & Suchard, M. A. (2013). Improving Bayesian population dynamics inference: a coalescent-based model for multiple loci. *Molecular Biology and Evolution*, 30(3), 713–724.
- Gordon, A., Hannon, G. J., & Others. (2010). *Fastx-toolkit*. FASTQ/A Short-Reads Preprocessing Tools (unpublished) [http://hannonlab.Cshl.Edu/fastx\\_toolkit,5](http://hannonlab.Cshl.Edu/fastx_toolkit,5).
- Green, R. E., Krause, J., Briggs, A. W., Maricic, T., Stenzel, U., Kircher, M., Patterson, N., Li, H., Zhai, W., Hsi-Yang Fritz, M., Hansen, N. F., Durand, E. Y., Malaspina, A.-S., Jensen, J. D., Marques-Bonet, T., Alkan, C., Prüfer, K., Meyer, M., Burbano, H. A., ... Pääbo, S. (2010). A draft sequence of the Neandertal genome. *Science*, 328(5979), 710–722.
- Gronau, I., Hubisz, M. J., Gulko, B., Danko, C. G., & Siepel, A. (2011). Bayesian inference of ancient human demography from individual genome sequences. *Nature Genetics*, 43(10), 1031–1034.
- Guthrie, R. D. (1982). Mammals of the mammoth steppe as paleoenvironmental indicators. In D. M. Hopkins, J. V. Matthews, C. E. Schweger, & S. B. Young (Eds.), *Paleoecology of Beringia* (pp. 307–326). Academic Press.
- Guthrie, R. D. (2001). Origin and causes of the mammoth steppe: a story of cloud cover, woolly mammal tooth pits, buckles, and inside-out Beringia. *Quaternary Science Reviews*, 20(1), 549–574.
- Guthrie, R. D. (2006). New carbon dates link climatic change with human colonization and Pleistocene extinctions. *Nature*, 441(7090), 207–209.
- Haile, J., Froese, D. G., MacPhee, R. D. E., Roberts, R. G., Arnold, L. J., Reyes, A. V., Rasmussen, M., Nielsen, R., Brook, B. W., Robinson, S., Demuro, M., Gilbert, M. T. P., Munch, K., Austin, J. J., Cooper, A., Barnes, I., Möller, P., & Willerslev, E. (2009). Ancient DNA reveals late survival of mammoth and horse in interior Alaska. *Proceedings of the National Academy of Sciences of the United States of America*, 106(52), 22352–22357.
- Heintzman, P. D., Zazula, G. D., MacPhee, R. D. E., Scott, E., Cahill, J. A., McHorse, B. K., Kapp, J. D., Stiller, M., Wooller, M. J., Orlando, L., Southon, J., Froese, D. G., & Shapiro, B. (2017). A new genus of horse from Pleistocene North America. *eLife*, 6, 1–43. <https://doi.org/10.7554/eLife.29944>.
- Hill, V., & Baele, G. (2019). Bayesian estimation of past population dynamics in BEAST 1.10 using the skygrid coalescent model. *Molecular Biology and Evolution*, 36(11), 2620–2628.

- Hopkins, D. M. (1959). Cenozoic History of the Bering Land Bridge: The seaway between the Pacific and Arctic basins has often been a land route between Siberia and Alaska. *Science*, 129, 1519–1528. <https://doi.org/10.1126/science.129.3362.1519>.
- Hopkins, D. M. (1973). Sea level history in beringia during the past 250,000 years. *Quaternary Research*, 3(4), 520–540.
- Hu, A., Meehl, G. A., Han, W., Timmermann, A., Otto-Bliesner, B., Liu, Z., Washington, W. M., Large, W., Abe-Ouchi, A., Kimoto, M., Lambeck, K., & Wu, B. (2012). Role of the Bering Strait on the hysteresis of the ocean conveyor belt circulation and glacial climate stability. *Proceedings of the National Academy of Sciences of the United States of America*, 109(17), 6417–6422.
- Hu, A., Meehl, G. A., Otto-Bliesner, B. L., Waelbroeck, C., Han, W., Loutre, M.-F., Lambeck, K., Mitrovica, J. X., & Rosenbloom, N. (2010). Influence of Bering Strait flow and North Atlantic circulation on glacial sea-level changes. *Nature Geoscience*, 3(2), 118–121.
- Irizarry, R. A., Wu, H., & Feinberg, A. P. (2009). A species-generalized probabilistic model-based definition of CpG islands. *Mammalian Genome*, 20(9–10), 674–680.
- Jakobsson, M., Pearce, C., Cronin, T. M., Backman, J., Anderson, L. G., Barrientos, N., Björk, G., Coxall, H., Boer, A., Mayer, L. A., Mörth, C.-M., Nilsson, J., Rattray, J. E., Stranne, C., Semiletov, I. & O'Regan, M. (2017). Post-glacial flooding of the Bering Land Bridge dated to 11 cal ka BP based on new geophysical and sediment records. *Climate of the past*, 13(8), 991–1005.
- Jónsson, H., Ginolhac, A., Schubert, M., Johnson, P. L. F., & Orlando, L. (2013). mapDamage2.0: fast approximate Bayesian estimates of ancient DNA damage parameters. *Bioinformatics*, 29(13), 1682–1684.
- Juric, I., Aeschbacher, S., & Coop, G. (2016). The strength of selection against neanderthal introgression. *PLoS Genetics*, 12(11), e1006340.
- Kapp, J. D., Green, R. E., & Shapiro, B. (2020). *A fast and efficient single-stranded genomic library preparation method optimized for ancient DNA*. Manuscript Submitted for Publication.
- Karolchik, D., Hinrichs, A. S., Furey, T. S., Roskin, K. M., Sugnet, C. W., Haussler, D., & Kent, W. J. (2004). The UCSC Table Browser data retrieval tool. *Nucleic Acids Research*, 32(Database issue), D493–D496.
- Kassambara, A., & Mundt, F. (2017). Factoextra: extract and visualize the results of multivariate data analyses. *R Package Version*, 1(4), 2017.
- Kircher, M., Sawyer, S., & Meyer, M. (2012). Double indexing overcomes inaccuracies in multiplex sequencing on the Illumina platform. *Nucleic Acids Research*, 40(1), e3.
- Knebel, H. J., & Creager, J. S. (1973). Yukon river: Evidence for extensive migration during the holocene transgression. *Science*, 179(4079), 1230–1232.
- Korlević, P., & Meyer, M. (2019). Pretreatment: Removing DNA Contamination from Ancient Bones and Teeth Using Sodium Hypochlorite and Phosphate. In B. Shapiro, A. Barlow, P. D. Heintzman, M. Hofreiter, J. L. A. Pajmians, & A. E. R. Soares (Eds.), *Ancient DNA: Methods and Protocols* (pp. 15–19). Springer New York.
- Korneliussen, T. S., Albrechtsen, A., & Nielsen, R. (2014). ANGSD: Analysis of next generation sequencing data. *BMC Bioinformatics*, 15, 356.
- Li, H. (2011). A statistical framework for SNP calling, mutation discovery, association mapping and population genetical parameter estimation from sequencing data. *Bioinformatics*, 27(21), 2987–2993.
- Li, H., & Durbin, R. (2009). Fast and accurate short read alignment with Burrows-Wheeler transform. *Bioinformatics*, 25(14), 1754–1760.
- Li, H., & Durbin, R. (2011). Inference of human population history from individual whole-genome sequences. *Nature*, 475(7357), 493–496.
- Li, H., Handsaker, B., Wysoker, A., Fennell, T., Ruan, J., Homer, N., Marth, G., Abecasis, G., & Durbin, R., 1000 Genome Project Data Processing Subgroup (2009). The sequence alignment/map format and SAMtools. *Bioinformatics*, 25(16), 2078–2079.
- Librado, P., Der Sarkissian, C., Ermini, L., Schubert, M., Jónsson, H., Albrechtsen, A., Fumagalli, M., Yang, M. A., Gamba, C., Seguin-Orlando, A., Mortensen, C. D., Petersen, B., Hoover, C. A., Lorente-Galdos, B., Nédoluzhko, A., Boulygina, E., Tsygankova, S., Neuditschko, M., Jagannathan, V., ... Orlando, L. (2015). Tracking the origins of Yakutian horses and the genetic basis for their fast adaptation to subarctic environments. *Proceedings of the National Academy of Sciences of the United States of America*, 112(50), E6889–E6897.
- Librado, P., Gamba, C., Gaunitz, C., Der Sarkissian, C., Pruvost, M., Albrechtsen, A., Fages, A., Khan, N., Schubert, M., Jagannathan, V., Serres-Armero, A., Kuderna, L. F. K., Povolotskaya, I. S., Seguin-Orlando, A., Lepetz, S., Neuditschko, M., Thèves, C., Alquraishi, S., Alfarhan, A. H., ... Orlando, L. (2017). Ancient genomic changes associated with domestication of the horse. *Science*, 356(6336), 442–445.
- Librado, P., & Orlando, L. (2020). Genomics and the evolutionary history of equids. *Annual Review of Animal Biosciences*, 9(1), 81–101. <https://doi.org/10.1146/annurev-animal-061220-023118>.
- Lippold, S., Matzke, N. J., Reissmann, M., & Hofreiter, M. (2011). Whole mitochondrial genome sequencing of domestic horses reveals incorporation of extensive wild horse diversity during domestication. *BMC Evolutionary Biology*, 11, 328.
- Lisiecki, L. E., & Raymo, M. E. (2005). A Pliocene-Pleistocene stack of 57 globally distributed benthic  $\delta^{18}O$  records. *Paleoceanography*, 20(1), 1–17. <https://doi.org/10.1029/2004PA001071>.
- Lister, A. M., & Sher, A. V. (2015). Evolution and dispersal of mammoths across the Northern Hemisphere. *Science*, 350(6262), 805–809.
- Loog, L., Thalmann, O., Sinding, M.-H.-S., Schuenemann, V. J., Perri, A., Geronpré, M., Bocherens, H., Witt, K. E., Samaniego Castruita, J. A., Velasco, M. S., Lundström, I. K. C., Wales, N., Sonet, G., Frantz, L., Schroeder, H., Budd, J., Jimenez, E.-L., Fedorov, S., Gasparyan, B., ... Manica, A. (2019). Ancient DNA suggests modern wolves trace their origin to a Late Pleistocene expansion from Beringia. *Molecular Ecology*, 29(9), 1596–1610. <https://doi.org/10.1111/mec.15329>.
- Lorenzen, E. D., Nogués-Bravo, D., Orlando, L., Weinstock, J., Binladen, J., Marske, K. A., Ugan, A., Borregaard, M. K., Gilbert, M. T. P., Nielsen, R., Ho, S. Y. W., Goebel, T., Graf, K. E., Byers, D., Stenderup, J. T., Rasmussen, M., Campos, P. F., Leonard, J. A., Koepfli, K.-P., Froese, D., Zazula, G., Stafford, T. W., Aaris-Sørensen, K., Batra, P., Haywood, A. M., Singarayer, J. S., Valdes, P. J., Boeskorov, G., Burns, J. A., Davydov, S. P., Haile, J., Jenkins, D. L., Kosintsev, P., Kuznetsova, T., Lai, X., Martin, L. D., Gregory McDonald, H., Mol, D., Meldgaard, M., ... Willerslev, E. (2011). Species-specific responses of Late Quaternary megafauna to climate and humans. *Nature*, 479(7373), 359–364.
- MacFadden, B. J. (2005). Fossil horses - evidence for evolution. *Science*, 307(5716), 1728–1730.
- Mann, D. H., Groves, P., Reanier, R. E., Gaglioti, B. V., Kunz, M. L., & Shapiro, B. (2015). Life and extinction of megafauna in the ice-age Arctic. *Proceedings of the National Academy of Sciences of the United States of America*, 112(46), 14301–14306.
- Marques, D. A., Lucek, K., Sousa, V. C., Excoffier, L., & Seehausen, O. (2019). Admixture between old lineages facilitated contemporary ecological speciation in Lake Constance stickleback. *Nature Communications*, 10(1), 4240.
- McKenna, A., Hanna, M., Banks, E., Sivachenko, A., Cibulskis, K., Kernysky, A., Garimella, K., Altshuler, D., Gabriel, S., Daly, M., & DePristo, M. A. (2010). The Genome Analysis Toolkit: a MapReduce framework for analyzing next-generation DNA sequencing data. *Genome Research*, 20(9), 1297–1303.
- McKeon, C. S., Weber, M. X., Alter, S. E., Seavy, N. E., Crandall, E. D., Barshis, D. J., Fechter-Leggett, E. D., & Oleson, K. L. L. (2016). Melting barriers to faunal exchange across ocean basins. *Global Change Biology*, 22(2), 465–473.
- Meiri, M., Lister, A. M., Collins, M. J., Tuross, N., Goebel, T., Blockley, S., Zazula, G. D., van Doorn, N., Dale Guthrie, R., Boeskorov, G. G., Baryshnikov, G. F., Sher, A., & Barnes, I. (2014). Faunal



- record identifies Bering isthmus conditions as constraint to end-Pleistocene migration to the New World. *Proceedings. Biological Sciences / the Royal Society*, 281(1776), 20132167.
- Meiri, M., Lister, A., Kosintsev, P., Zazula, G., & Barnes, I. (2020). Population dynamics and range shifts of moose (*Alces alces*) during the Late Quaternary. *Journal of Biogeography*, 47(10), 2223–2234.
- Meisner, J., & Albrechtsen, A. (2018). Inferring population structure and admixture proportions in low-depth NGS data. *Genetics*, 210(2), 719–731.
- Meyer, M., & Kircher, M. (2010). Illumina sequencing library preparation for highly multiplexed target capture and sequencing. *Cold Spring Harbor Protocols*, 2010(6), db.prot5448.
- Minin, V. N., & Suchard, M. A. (2008a). Counting labeled transitions in continuous-time Markov models of evolution. *Journal of Mathematical Biology*, 56(3), 391–412.
- Minin, V. N., & Suchard, M. A. (2008b). Fast, accurate and simulation-free stochastic mapping. *Philosophical Transactions of the Royal Society of London. Series B, Biological Sciences*, 363(1512), 3985–3995.
- Moreno-Mayar, J. V., Potter, B. A., Vinner, L., Steinrücken, M., Rasmussen, S., Terhorst, J., Kamm, J. A., Albrechtsen, A., Malaspina, A.-S., Sikora, M., Reuther, J. D., Irish, J. D., Malhi, R. S., Orlando, L., Song, Y. S., Nielsen, R., Meltzer, D. J., & Willerslev, E. (2018). Terminal Pleistocene Alaskan genome reveals first founding population of Native Americans. *Nature*, 553(7687), 203–207.
- Nielsen, R., Paul, J. S., Albrechtsen, A., & Song, Y. S. (2011). Genotype and SNP calling from next-generation sequencing data. *Nature Reviews. Genetics*, 12(6), 443–451.
- Nosil, P., & Feder, J. L. (2012). Genomic divergence during speciation: causes and consequences. *Philosophical Transactions of the Royal Society of London. Series B, Biological Sciences*, 367(1587), 332–342.
- O'Regan, M., John, K. S., Moran, K., Backman, J., King, J., Haley, B. A., Jakobsson, M., Frank, M., Röhl, U. (2010). Plio-Pleistocene trends in ice rafted debris on the Lomonosov Ridge. *Quaternary International: the Journal of the International Union for Quaternary Research*, 219(1), 168–176.
- Orlando, L. (2020). Ancient Genomes Reveal Unexpected Horse Domestication and Management Dynamics. *BioEssays: News and Reviews in Molecular, Cellular and Developmental Biology*, 42(1), e1900164.
- Orlando, L., Ginolhac, A., Zhang, G., Froese, D., Albrechtsen, A., Stiller, M., Schubert, M., Cappellini, E., Petersen, B., Moltke, I., Johnson, P. L. F., Fumagalli, M., Vilstrup, J. T., Raghavan, M., Korneliusen, T., Malaspina, A.-S., Vogt, J., Szklarczyk, D., Kelstrup, C. D., ... Willerslev, E. (2013). Recalibrating Equus evolution using the genome sequence of an early Middle Pleistocene horse. *Nature*, 499(7456), 74–78.
- Orr, H. A., Masly, J. P., & Presgraves, D. C. (2004). Speciation genes. *Current Opinion in Genetics & Development*, 14(6), 675–679.
- Orr, H. A., & Presgraves, D. C. (2000). Speciation by postzygotic isolation: forces, genes and molecules. *BioEssays: News and Reviews in Molecular, Cellular and Developmental Biology*, 22(12), 1085–1094.
- Quedraogo, M., Bettembourg, C., Bretaudeau, A., Sallou, O., Diot, C., Demeure, O., & Lecerf, F. (2012). The duplicated genes database: identification and functional annotation of co-localised duplicated genes across genomes. *PLoS One*, 7(11), e50653.
- Patten, M. A. (2015). Subspecies and the philosophy of science. *The Auk: Ornithological Advances*, 132(2), 481–485.
- Payseur, B. A., & Rieseberg, L. H. (2016). A genomic perspective on hybridization and speciation. *Molecular Ecology*, 25(11), 2337–2360.
- Pease, J. B., & Hahn, M. W. (2015). Detection and polarization of introgression in a five-taxon phylogeny. *Systematic Biology*, 64(4), 651–662.
- Quinlan, A. R., & Hall, I. M. (2010). BEDTools: a flexible suite of utilities for comparing genomic features. *Bioinformatics*, 26(6), 841–842.
- R Core Team (2014). *R: A Language and Environment for Statistical Computing*. R Foundation for Statistical Computing. Retrieved from <http://www.R-project.org/>.
- Rambaut, A., & Drummond, A. J. (2010). *TreeAnnotator version, Vol. 1* (p. 1). University of Edinburgh. Retrieved from [https://scholar.google.ca/scholar?cluster=16034997356612446945&hl=en&as\\_sdt=0.5&scioldt=0.5](https://scholar.google.ca/scholar?cluster=16034997356612446945&hl=en&as_sdt=0.5&scioldt=0.5).
- Rambaut, A., Drummond, A. J., Xie, D., Baele, G., & Suchard, M. A. (2018). Posterior Summarization in Bayesian Phylogenetics Using Tracer 1.7. *Systematic Biology*, 67(5), 901–904.
- Ramsey, C. B. (2009). Bayesian analysis of radiocarbon dates. *Radiocarbon*, 51(1), 337–360. <https://doi.org/10.1017/S0033822200033865>.
- Rasmussen, M., Guo, X., Wang, Y., Lohmueller, K. E., Rasmussen, S., Albrechtsen, A., Skotte, L., Lindgreen, S., Metspalu, M., Jombart, T., Kivisild, T., Zhai, W., Eriksson, A., Manica, A., Orlando, L., De La Vega, F. M., Tridico, S., Metspalu, E., Nielsen, K., ... Willerslev, E. (2011). An Aboriginal Australian genome reveals separate human dispersals into Asia. *Science*, 334(6052), 94–98.
- Reimer, P. J., Bard, E., Bayliss, A., Beck, J. W., Blackwell, P. G., Ramsey, C. B., Buck, C. E., Cheng, H., Edwards, R. L., Friedrich, M., Grootes, P. M., Guilderson, T. P., Hafldason, H., Hajdas, I., Hatté, C., Heaton, T. J., Hoffmann, D. L., Hogg, A. G., Hughen, K. A., ... van der Plicht, J. (2013). IntCal13 and marine13 radiocarbon age calibration curves 0–50,000 years cal BP. *Radiocarbon*, 55(4), 1869–1887. [http://doi.org/10.2458/azu\\_js\\_rc.55.16947](http://doi.org/10.2458/azu_js_rc.55.16947).
- Rohland, N., Reich, D., Mallick, S., Meyer, M., Green, R. E., Georgiadis, N. J., Roca, A. L., Hofreiter, M. (2010). Genomic DNA sequences from mastodon and woolly mammoth reveal deep speciation of forest and savanna elephants. *PLoS Biology*, 8(12), e1000564.
- Saarela, J., Cirilli, O., Strani, F., Meshida, K., & Bernor, R. L. (2021). Testing equid body mass estimate equations on modern zebras—with implications to understanding the relationship of body size, diet, and habitats of equus in the pleistocene of Europe. *Frontiers in Ecology and Evolution*, 9, 90.
- Salis, A. T., Bray, S. C. E., Lee, M. S. Y., Heiniger, H., Barnett, R., Burns, J. A., Mitchell, K. J. (2020). *Lions and brown bears colonized North America in multiple synchronous waves of dispersal across the Bering Land Bridge* (p. 2020.09.03.279117). <https://doi.org/10.1101/2020.09.03.279117>
- Savolainen, O., Lascoux, M., & Merilä, J. (2013). Ecological genomics of local adaptation. *Nature Reviews Genetics*, 14(11), 807–820.
- Schild, D. R., Perry, B. W., Adams, R. H., Card, D. C., Jezkova, T., Pasquesi, G. I. M., Nikolakis, Z. L., Row, K., Meik, J. M., Smith, C. F., Mackessy, S. P., Castoe, T. A. (2019). Allopatric divergence and secondary contact with gene flow: a recurring theme in rattlesnake speciation. *Biological Journal of the Linnean Society. Linnean Society of London*, 128(1), 149–169.
- Schmieder, R., & Edwards, R. (2011). Quality control and preprocessing of metagenomic datasets. *Bioinformatics*, 27(6), 863–864.
- Schubert, M., Ginolhac, A., Lindgreen, S., Thompson, J. F., Al-Rasheid, K. A. S., Willerslev, E., & Orlando, L. (2012). Improving ancient DNA read mapping against modern reference genomes. *BMC Genomics*, 13, 178.
- Schubert, M., Jónsson, H., Chang, D., Der Sarkissian, C., Ermini, L., Ginolhac, A., Albrechtsen, A., Dupanloup, I., Foucal, A., Petersen, B., Fumagalli, M., Raghavan, M., Seguin-Orlando, A., Korneliusen, T. S., Velazquez, A. M. V., Stenderup, J., Hoover, C. A., Rubin, C.-J., Alfarhan, A. H., ... Orlando, L. (2014). Prehistoric genomes reveal the genetic foundation and cost of horse domestication. *Proceedings of the National Academy of Sciences of the United States of America*, 111(52), E5661–E5669.
- Sher, A. (1999). Traffic lights at the Beringian crossroads. *Nature*, 397(6715), 103–104.
- Smit, A. F. A., Hubley, R., & Green, P. (2013–2015). *RepeatMasker Open-4.0*. Retrieved from <http://www.repeatmasker.org>

- South, A. (2011). rworldmap: A New R package for Mapping Global Data. *The R Journal*, 3, 35–43. Retrieved from [http://journal.r-project.org/archive/2011-1/RJournal\\_2011-1\\_South.pdf](http://journal.r-project.org/archive/2011-1/RJournal_2011-1_South.pdf).
- Stamatakis, A. (2014). RAxML version 8: a tool for phylogenetic analysis and post-analysis of large phylogenies. *Bioinformatics*, 30(9), 1312–1313.
- Stuart, A. J., & Lister, A. M. (2012). Extinction chronology of the woolly rhinoceros *Coelodonta antiquitatis* in the context of late Quaternary megafaunal extinctions in northern Eurasia. *Quaternary Science Reviews*, 51, 1–17.
- Suchard, M. A., Lemey, P., Baele, G., Ayres, D. L., Drummond, A. J., & Rambaut, A. (2018). Bayesian phylogenetic and phylodynamic data integration using BEAST 1.10. *Virus Evolution*, 4(1), vey016.
- Turelli, M., & Orr, H. A. (2000). Dominance, epistasis and the genetics of postzygotic isolation. *Genetics*, 154(4), 1663–1679.
- Vershinina, A. O., Kapp, J. D., Baryshnikov, G. F., & Shapiro, B. (2019). The case of an arctic wild ass highlights the utility of ancient DNA for validating problematic identifications in museum collections. *Molecular Ecology Resources*, 20(5), 1182–1190. <https://doi.org/10.1111/1755-0998.13130>.
- Vilstrup, J. T., Seguin-Orlando, A., Stiller, M., Ginolhac, A., Raghavan, M., Nielsen, S. C. A., Weinstock, J., Froese, D., Vasiliev, S. K., Ovodov, N. D., Clary, J., Helgen, K. M., Fleischer, R. C., Cooper, A., Shapiro, B., & Orlando, L. (2013). Mitochondrial phylogenomics of modern and ancient equids. *PLoS One*, 8(2), e55950.
- Vitti, J. J., Grossman, S. R., & Sabeti, P. C. (2013). Detecting natural selection in genomic data. *Annual Review of Genetics*, 47, 97–120.
- Wade, C. M., Giulotto, E., Sigurdsson, S., Zoli, M., Gnerre, S., Imsland, F., Lear, T. L., Adelson, D. L., Bailey, E., Bellone, R. R., Blöcker, H., Distl, O., Edgar, R. C., Garber, M., Leeb, T., Mauceli, E., MacLeod, J. N., Penedo, M. C., Raison, J. M., ... Lindblad-Toh, K. (2009). Genome sequence, comparative analysis, and population genetics of the domestic horse. *Science*, 326(5954), 865–867.
- Wang, L.-G., Lam, T.-T.-Y., Xu, S., Dai, Z., Zhou, L., Feng, T., Guo, P., Dunn, C. W., Jones, B. R., Bradley, T., Zhu, H., Guan, Y. I., Jiang, Y., & Yu, G. (2020). Treeio: An R Package for Phylogenetic Tree Input and Output with Richly Annotated and Associated Data. *Molecular Biology and Evolution*, 37(2), 599–603.
- Weinstock, J., Willerslev, E., Sher, A., Tong, W., Ho, S. Y. W., Rubenstein, D., Storer, J., Burns, J., Martin, L., Bravi, C., Prieto, A., Froese, D., Scott, E., Xulong, L., & Cooper, A. (2005). Evolution, systematics, and phylogeography of pleistocene horses in the new world: a molecular perspective. *PLoS Biology*, 3(8), e241.
- Wickham, H. (2016). *ggplot2: Elegant Graphics for Data Analysis*. Springer-Verlag. Retrieved from <https://ggplot2.tidyverse.org>.
- Wooller, M. J., Saulnier-Talbot, É., Potter, B. A., Belmecheri, S., Bigelow, N., Choy, K., Cwynar, L. C., Davies, K., Graham, R. W., Kurek, J., Langdon, P., Medeiros, A., Rawcliffe, R., Wang, Y., & Williams, J. W. (2018). A new terrestrial palaeoenvironmental record from the Bering Land Bridge and context for human dispersal. *Royal Society Open Science*, 5(6), 180145.
- Wu, H., Caffo, B., Jaffee, H. A., Irizarry, R. A., & Feinberg, A. P. (2010). Redefining CpG islands using hidden Markov models. *Biostatistics*, 11(3), 499–514.
- Xu, X., & Arnason, U. (1994). The complete mitochondrial DNA sequence of the horse, *Equus caballus*: extensive heteroplasmy of the control region. *Gene*, 148(2), 357–362.
- Xu, X., Gullberg, A., & Arnason, U. (1996). The complete mitochondrial DNA (mtDNA) of the donkey and mtDNA comparisons among four closely related mammalian species-pairs. *Journal of Molecular Evolution*, 43(5), 438–446.
- Yates, A. D., Achuthan, P., Akanni, W., Allen, J., Allen, J., Alvarez-Jarreta, J., Ridwan Amode, M., Armean, I. M., Azov, A. G., Bennett, R., Bhai, J., Billis, K., Boddu, S., Carlos Marugán, J., Cummins, C., Davidson, C., Dodiya, K., Fatima, R., Gall, A., Garcia Giron, C., Gil, L., Grego, T., Haggerty, L., Haskell, E., Hourlier, T., Izuogu, O. G., Janacek, S. H., Juettemann, T., Kay, M., Lavidas, I., Le, T., Lemos, D., Gonzalez Martinez, J., Maurel, T., McDowall, M., McMahon, A., Mohanan, S., Moore, B., Nuhn, M., Oheh, D. N., Parker, A., Parton, A., Patricio, M., Sakthivel, M. P. ... Flicek, P. (2020). Ensembl 2020. *Nucleic Acids Research*, 48(D1), D682–D688.
- Yu, G., Smith, D. K., Zhu, H., Guan, Y., & Lam, T.-T.-Y. (2017). ggtree: an R package for visualization and annotation of phylogenetic trees with their covariates and other associated data. *Methods in Ecology and Evolution* / *British Ecological Society*, 8(1), 28–36.
- Yuan, J., Sheng, G., Preick, M., Sun, B., Hou, X., Chen, S., Taron, U. H., Barlow, A., Wang, L., Hu, J., Deng, T., Lai, X., & Hofreiter, M. (2020). Mitochondrial genomes of Late Pleistocene caballine horses from China belong to a separate clade. *Quaternary Science Reviews*, 250, 106691.
- Zazula, G. D., MacPhee, R. D. E., Metcalfe, J. Z., Reyes, A. V., Brock, F., Druckenmiller, P. S., Groves, P., Harington, C. R., Hodgins, G. W. L., Kunz, M. L., Longstaffe, F. J., Mann, D. H., McDonald, H. G., Nalawade-Chavan, S., & Southon, J. R. (2014). American mastodon extirpation in the Arctic and Subarctic predates human colonization and terminal Pleistocene climate change. *Proceedings of the National Academy of Sciences of the United States of America*, 111(52), 18460–18465.
- Zheng, Y., & Janke, A. (2018). Gene flow analysis method, the D-statistic, is robust in a wide parameter space. *BMC Bioinformatics*, 19(1), 10.
- Zhou, B., Wen, S., Wang, L., Jin, L., Li, H., & Zhang, H. (2017). AntCaller: an accurate variant caller incorporating ancient DNA damage. *Molecular Genetics and Genomics: MGG*, 292(6), 1419–1430.
- Zimov, S. A., Zimov, N. S., Tikhonov, A. N., & Chapin, F. S. (2012). Mammoth steppe: a high-productivity phenomenon. *Quaternary Science Reviews*, 57, 26–45.

## SUPPORTING INFORMATION

Additional supporting information may be found online in the Supporting Information section.

**How to cite this article:** Vershinina AO, Heintzman PD, Froese DG, et al. Ancient horse genomes reveal the timing and extent of dispersals across the Bering Land Bridge. *Mol Ecol*. 2021;30:6144–6161. <https://doi.org/10.1111/mec.15977>